PD IEC TS 62882:2020



BSI Standards Publication

Hydraulic machines — Francis turbine pressure fluctuation transposition

Documents
Document Sharing Hub

Full document details: PD IEC TS 62882:2020

National foreword

This Published Document is the UK implementation of IEC TS 62882:2020.

The UK participation in its preparation was entrusted to Technical Committee MCE/15, Hydraulic turbines.

A list of organizations represented on this committee can be obtained on request to its committee manager.

This publication does not purport to include all the necessary provisions of a contract. Users are responsible for its correct application.

© The British Standards Institution 2020
Published by BSI Standards Limited 2020

ISBN 978 0 539 01937 7

ICS 27.140

Compliance with a British Standard cannot confer immunity from legal obligations.

This Published Document was published under the authority of the Standards Policy and Strategy Committee on 30 September 2020.

Amendments/corrigenda issued since publication

Date	Text affected

Documents
Document Sharing Hub

Full document details: PD IEC TS 62882:2020

IEC TS 62882

Edition 1.0 2020-09

TECHNICAL SPECIFICATION

colour inside

Hydraulic machines – Francis turbine pressure fluctuation transposition

INTERNATIONAL
ELECTROTECHNICAL
COMMISSION

ICS 27.140

ISBN 978-2-8322-8786-6

Warning! Make sure that you obtained this publication from an authorized distributor.

® Registered trademark of the International Electrotechnical Commission

Documents
Document Sharing Hub

Full document details: PD IEC TS 62882:2020

CONTENTS

FOREWORD 9
INTRODUCTION 11
1 Scope 12
2 Normative references 13
3 Terms, definitions, symbols and units 13
3.1 General terms and definitions 13
3.2 Units 13
3.3 Overview of the terms, definitions, symbols and units used in this document 14
3.3.1 Subscripts and symbols 15
3.3.2 Geometric terms and definitions 16
3.3.3 Physical quantities and properties terms and definitions 17
3.3.4 Discharge, velocity and speed terms and definitions 17
3.3.5 Pressure terms and definitions 18
3.3.6 Specific energy terms and definitions 18
3.3.7 Height and head terms and definitions 19
3.3.8 Power and torque terms and definitions 20
3.3.9 Efficiency terms and definitions 21
3.3.10 General terms and definitions relating to fluctuating quantities 21
3.3.11 Fluid dynamic and scaling terms and definitions 24
3.3.12 Dimensionless terms and definitions 24
4 Description of pressure fluctuation phenomena 25
4.1 General 25
4.2 Pressure fluctuations overview 30
4.3 General description of draft tube flow in Francis turbines 32
4.4 Detailed description of pressure fluctuation phenomena 34
4.4.1 Mode 1: Pressure fluctuation in high load 34
4.4.2 Mode 2: Pressure fluctuation in best operation range 35
4.4.3 Mode 3: Pressure fluctuation in upper part load 35
4.4.4 Mode 4: Pressure fluctuation in part load 36
4.4.5 Mode 5: Pressure fluctuation in deep part load 38
4.4.6 Modes 6.a and 6.b: Rotor-stator interaction (RSI) pressure fluctuation 39
5 Specifications of pressure fluctuation measurement and analysis 41
5.1 General 41
5.1.1 Overview 41
5.1.2 Purpose of the measurements 41
5.1.3 Procedures and parameters to record 42
5.1.4 Locations of pressure fluctuation test transducers 43
5.1.5 Data acquisition for pressure fluctuation measurements 44
5.1.6 Transducers and calibration 45
5.2 Pressure fluctuation on a model turbine 45
5.2.1 General 45
5.2.2 Homology and limitations 46
5.2.3 Detailed procedures 46
5.3 Special requirements and information for a prototype turbine 48
5.3.1 General 48
5.3.2 Source of information 48

AVA Documents
Document Sharing Hub

Full document details: PD IEC TS 62882:2020

5.3.3 Important aspects 48
5.4 Analysis, presentation and interpretation of results 49
5.4.1 General 49
5.4.2 Time-domain analysis 49
5.4.3 Frequency-domain analysis 50
5.4.4 Non-dimensional frequency and pressure 50
5.4.5 Presentation and interpretation of pressure fluctuations 50
6 Identification of potential resonances in test rig and prototype 51
6.1 General 51
6.2 Identify resonance in test rig 53
6.3 Possible resonance and self-excited pressure fluctuation in prototype 53
6.3.1 General 53
6.3.2 Draft tube vortex related resonances and self-excited pressure fluctuation in prototype 53
6.3.3 Rotor-stator interaction (RSI) related resonance 55
6.3.4 Resonance with fluctuation modes not treated in this document 55
7 Transposition method and procedure 56
7.1 General 56
7.2 Parameters influencing transposition 56
7.2.1 Model test head 56
7.2.2 Thoma number 56
7.2.3 Froude number 57
7.3 Relevant quantities for transposition 57
7.3.1 Fluctuation frequency 57
7.3.2 Fluctuation amplitude 57
7.4 Transposable types of fluctuations 57
7.5 Statistical analysis of model and prototype transposition accuracy 58
8 Mitigations 59
8.1 Draft tube vortex phenomena 59
8.1.1 General 59
8.1.2 Draft tube fins 59
8.1.3 Draft tube with a central column 60
8.1.4 Air admission 61
8.1.5 AVR or PSS parameter tuning 62
8.2 Runner inter-blade vortex 63
8.3 Blade interaction 63
8.4 Operation restriction 63
Annex A (informative) Example of pressure fluctuation records 64
Annex B (informative) Typical pressure fluctuation transducers parameters for model test 83
Annex C (informative) Pressure transducer dynamic calibration 84
C.1 Fast valve opening method 84
C.2 Rotating valve method 84
C.3 Electrical spark method 85
Annex D (informative) Proposed remote pressure measurement fluctuation correction 86
D.1 General 86
D.2 Correction method theory 86
D.3 Measuring and estimating tube frequency response 87

AVA Documents
Document Sharing Hub

Full document details: PD IEC TS 62882:2020

D.4 Pressure fluctuation correction 89
D.5 Limitations 92
Annex E (informative) Forced response analysis for Francis turbines operating in part load conditions 93
E.1 General 93
E.2 Systematic methodology based on detailed modelling of hydroelectric power plant 93
E.2.1 Description of the test case 93
E.2.2 Modelling of the hydraulic power plant 94
E.2.3 Forced response analysis of the test case 97
E.3 Simplified approach based on the hydroacoustic properties of the hydraulic system 100
E.3.1 General 100
E.3.2 Cavitating draft tube first natural frequency 100
E.3.3 Hydraulic circuit natural frequencies 101
E.3.4 Example of applications 102
E.3.5 Limitations of the methodology 107
Annex F (informative) Influence of Thoma number on pressure fluctuation 108
Annex G (informative) Transposition of synchronous pressure fluctuations from model to prototype for Francis turbines operating at off-design conditions 110
G.1 General 110
G.1.1 Overview 110
G.1.2 Step 1: 1-D numerical modelling of both the test rig at the model scale and the corresponding hydropower unit operating in off-design conditions 110
G.1.3 Step 2: Experimental identification of the parameters of interest on the reduced scale model 112
G.1.4 Step 3: Transposition of the hydroacoustic parameters from model to prototype 115
G.1.5 Step 4: Prediction of the precession frequency and eigenfrequencies at the prototype scale 116
G.1.6 Step 5: Prediction of pressure fluctuations at the prototype scale 116
G.2 Concluding remark: use of the local cavitation coefficient for transposition from model to prototype 116
Annex H (informative) Statistical analysis of pressure fluctuation data 119
H.1 Normalizing step for the comparison of data 119
H.2 Collected data 121
H.3 Draft tube zone phenomena 121
H.4 Vaneless zone phenomena 126
H.5 Spiral case phenomena 130
Annex J (informative) Gathering worldwide pressure fluctuation data 134
J.1 Chinese test cases 134
J.2 France test case 135
J.3 Norway test case 137
Bibliography 138

Figure 1 – Reference diameter of Francis turbine 16
Figure 2 – Reference level of the Francis turbine 19
Figure 3 – Flux diagram for power and discharge 20
Figure 4 – Illustration of some definitions related to fluctuating quantities 23

AVA Documents Document Sharing Hub

Full document details: PD IEC TS 62882:2020

Figure 5 – Discharge range for the various fluctuation modes 30
Figure 6 – Efficiency hill chart with pictures of swirling flow 31
Figure 7 – Example of a waterfall diagram of pressure amplitudes measured in the draft tube cone 32
Figure 8 – Velocity triangles at inlet and outlet of the runner blade 33
Figure 9 – Influence of the discharge on the circumferential component of the absolute velocity 34
Figure 10 – Elliptical vortex rope precessing in the draft tube cone at upper part load 36
Figure 11 – Decomposition between the synchronous and asynchronous component of part load draft tube pressure fluctuations 37
Figure 12 – Example of inter-blade vortex 38
Figure 13 – Modulation process between runner blade flow field and guide vanes flow field 39
Figure 14 – Diametrical modes shapes representation according to k values 40
Figure 15 – Suggested locations of pressure transducers 43
Figure 16 – Turbine hill-chart with exploration paths 45
Figure 17 – Schematic of the axial aeration device 47
Figure 18 – Schematic arrangement for pressure fluctuation transducers 49
Figure 19 – Typical plot showing pressure fluctuation coefficient versus relative discharge 51
Figure 20 – Elementary hydroacoustic oscillator 52
Figure 21 – Part load vortex rope in the draft tube and its fluctuation frequency range and corresponding risk of resonance with the generator local mode of oscillation valid for both F_{grid} = 50 Hz and F_{grid} = 60 Hz 54
Figure 22 – Waterfall diagram of the pressure fluctuations as function of the frequency and Froude number for a given Thoma number 57
Figure 23 – Example of fins in the draft tube and influence on the pressure fluctuations 60
Figure 24 – Example of the draft tube with central column extension 61
Figure 25 – Typical runner cone extensions used for reducing draft tube pressure fluctuations 61
Figure 26 – Central and peripheral air admission locations for draft tube pressure fluctuations on a radial flow turbine 62
Figure 27 – Central air admission 62
Figure A.1 – Example 1: a case corresponding to mode 1 (a limited high load) 66
Figure A.2 – Example 2: a case corresponding to mode 1 (a large overload) 68
Figure A.3 – Example 3: a case corresponding to mode 2 70
Figure A.4 – Example 4 : a case corresponding to mode 3 72
Figure A.5 – Example 5 : a case corresponding to mode 4.a and 4.b 74
Figure A.6 – Example 6: a case corresponding to mode 4.a and 4.b 76
Figure A.7 – Example 7: a case corresponding to mode 4.c 78
Figure A.8 – Example 8: a case corresponding to mode 5.b 80
Figure A.9 – Example 9: a case corresponding to mode 6.a 82
Figure C.1 – Pressure transducer dynamic calibration schematic diagram with fast open valve method 84
Figure C.2 – Pressure transducer dynamic calibration with rotating valve method 85

AVA Documents
Document Sharing Hub

Full document details: PD IEC TS 62882:2020

Figure C.3 – Spark plug used as to generate an impulse excitation in water for pressure transducer dynamic calibration 85
Figure D.1 – Typical results obtained by shutting off drainage valve 88
Figure D.2 – Signal and spectrum of four remote sensors and one local sensor 90
Figure D.3 – Signal and spectrum of four remote sensors (corrected) and one local sensor 91
Figure E.1 – SIMSEN model of the test case 94
Figure E.2 – Performance hill chart of the Francis turbine for different guide vane openings 94
Figure E.3 – Elementary hydraulic pipe of length dx and its equivalent circuit 96
Figure E.4 – Forced response for a = 50 m/s (left) and a = 60 m/s (right) 97
Figure E.5 – Forced response for a = 70 m/s (left) and a = 80 m/s (right) 98
Figure E.6 – Forced response for a = 90 m/s (left) and a = 100 m/s (right) 98
Figure E.7 – Damping and eigenfrequency for a = 50 m/s (left) and a = 60 m/s (right) 98
Figure E.8 – Damping and eigenfrequency for a = 70 m/s (left) and a = 80 m/s (right) 98
Figure E.9 – Damping and eigenfrequency for a = 90 m/s (left) and a = 100 m/s (right) 99
Figure E.10 – Eigenmode for a = 50 m/s and eigenfrequency f = 4,18 Hz 99
Figure E.11 – Eigenmode for a = 50 m/s and eigenfrequency f = 3,67 Hz 99
Figure E.12 – Eigenmode for a = 100 m/s and eigenfrequency f = 2,61 Hz 99
Figure E.13 – Draft tube modelled with cavitation compliance and draft tube inductance 100
Figure E.14 – Simplified model of a cavitation draft tube connected to a tailrace pipe composed by cavitation compliance of the draft tube and downstream inductance of the tailrace pipe 101
Figure E.15 – Hydraulic system modelled by an equivalent pipe and corresponding modes shapes for the first and second natural frequencies 102
Figure E.16 – Hydraulic systems 1, 2 and 3 103
Figure F.1 – Influence of Thoma number on pressure fluctuation 108
Figure F.2 – Example of waterfall diagram of the pressure fluctuations as function of the frequency and Thoma number 109
Figure G.1 – Peak-to-peak value of pressure fluctuations as a function of the discharge factor measured on the model and the corresponding prototype 110
Figure G.2 – Layout of EPFL test rig PF3 1-D hydroacoustic model 111
Figure G.3 – Electrical T-shaped representation of the cavitation vortex rope developing in Francis turbine draft tube in part load conditions 111
Figure G.4 – Excitation system and 3D cut-view of the rotating valve 113
Figure G.5 – Strouhal number of the precession frequency as a function of the swirl number computed with Formula (G.6) 114
Figure G.6 – Strouhal number of the first eigenfrequency of the test rig as a function of swirl number (a), the wave speed in the draft tube determined in the 1-D model (b) 115
Figure G.7 – Predicted values of precession frequency and first eigenfrequency at the prototype scale as a function of the output power of the generating unit 116
Figure G.8 – Comparison between observed and predicted values of the precession frequency f_{rope} and the first eigenfrequency f_0 of a 444 MW hydropower unit (HYPERBOLE project test case) 117
Figure G.9 – Hill chart comparing the measured and the predicted resonance conditions assuming a constant pressure value in the draft tube cone of the prototype 118
Figure H.1 – Pressure fluctuations versus discharge factor 120

AVA Documents
Document Sharing Hub

Full document details: PD IEC TS 62882:2020

Figure H.2 – Normalized discharge of pressure fluctuations 120
Figure H.3 – Normalized pressure amplitude of pressure fluctuations 120
Figure H.4 – Comparison of pressure fluctuations of model and prototype 120
Figure H.5 – Set of pressure fluctuation of models and prototypes for draft tube analysis 121
Figure H.6 – Difference between pressure fluctuations between the model and the prototype 122
Figure H.7 – Standard deviation of difference of pressure fluctuation 122
Figure H.8 – Transposition accuracy for draft tube cone 123
Figure H.9 – Transposition of each power plant test case for the draft tube cone 126
Figure H.10 – Set of pressure fluctuation of models and prototypes for vaneless zone analysis 127
Figure H.11 – Difference between pressure fluctuations between the model and the prototype 127
Figure H.12 – Standard deviation of difference of pressure fluctuation 128
Figure H.13 – Transposition accuracy for vaneless zone 128
Figure H.14 – Transposition of each power plant test case for vaneless zone 129
Figure H.15 – Set of pressure fluctuation of models and prototypes for spiral case analysis 130
Figure H.16 – Difference between pressure fluctuations between the model and the prototype 131
Figure H.17 – Standard deviation of difference of pressure fluctuation 131
Figure H.18 – Transposition accuracy for spiral case 132
Figure H.19 – Transposition of each power plant test cases for spiral case 133
Figure J.1 – Comparison of pressure fluctuations on the draft tube for 10 Chinese model and prototype references 135
Figure J.2 – Comparison of pressure fluctuations on the draft tube for one France model and prototype reference 136
Figure J.3 – Comparison of pressure fluctuations on the spiral case for one France model and prototype reference 136
Figure J.4 – Comparison of pressure fluctuations on the draft tube for one Norway model and prototype reference 137

Table 1 – Pressure fluctuation overview matrix 27
Table 2 – Locations of pressure fluctuations transducers 44
Table 3 – Accuracy for transposition of fluctuation amplitude in draft tube cone 58
Table 4 – Accuracy for transposition of fluctuation amplitude in vaneless zone 58
Table 5 – Accuracy for transposition of fluctuation amplitude in spiral case 59
Table D.1 – $f_{1/4}$ and dec calculated for p_1 to p_4 88
Table D.2 – Estimated frequencies based on tubing mechanical characteristics 89
Table D.3 – Peak-to-peak value on the raw signals 90
Table D.4 – Wave speed and damping ratio 90
Table D.5 – Peak-to-peak value on the corrected signals 92
Table E.1 – Francis turbine parameters 94
Table E.2 – Parameters of the hydraulic systems 1, 2 and 3 103
Table E.3 – Parameters of the equivalent pipe of the hydraulic system 1 104

AVA Documents
Document Sharing Hub

Full document details: PD IEC TS 62882:2020

Table E.4 – Estimation of the natural frequencies f_0 to f_6 of the hydraulic system 1 based on Formulae (E.9) and (E.11) and comparison with results obtained with eigenvalue calculation and corresponding errors 105
Table E.5 – Parameters of the equivalent pipe of the hydraulic system 2 105
Table E.6 – Estimation of the natural frequencies f_0 to f_6 of the hydraulic system 2 based on Formulae (E.10) and (E.11) and comparison with results obtained with eigenvalue calculation and corresponding errors 105
Table E.7 – Parameters of the equivalent pipe of the hydraulic system 3 106
Table E.8 – Estimation of the natural frequencies f_0 to f_6 of the hydraulic system 3 based on Formulae (E.10) and (E.11) and comparison with results obtained with eigenvalue calculation and corresponding errors 107
Table E.9 – Pressure mode shape obtained by eigenvalue and eigenvector calculation for the three first natural frequencies f_1, f_2 and f_3 of the hydraulic systems 1 and 2 107
Table H.1 – World hydropower plant references 121

Documents
Document Sharing Hub
Full document details: PD IEC TS 62882:2020

INTERNATIONAL ELECTROTECHNICAL COMMISSION

_____

HYDRAULIC MACHINES – FRANCIS TURBINE PRESSURE FLUCTUATION TRANSPOSITION

FOREWORD

1) The International Electrotechnical Commission (IEC) is a worldwide organization for standardization comprising all national electrotechnical committees (IEC National Committees). The object of IEC is to promote international co-operation on all questions concerning standardization in the electrical and electronic fields. To this end and in addition to other activities, IEC publishes International Standards, Technical Specifications, Technical Reports, Publicly Available Specifications (PAS) and Guides (hereafter referred to as "IEC Publication(s)"). Their preparation is entrusted to technical committees; any IEC National Committee interested in the subject dealt with may participate in this preparatory work. International, governmental and non-governmental organizations liaising with the IEC also participate in this preparation. IEC collaborates closely with the International Organization for Standardization (ISO) in accordance with conditions determined by agreement between the two organizations.
2) The formal decisions or agreements of IEC on technical matters express, as nearly as possible, an international consensus of opinion on the relevant subjects since each technical committee has representation from all interested IEC National Committees.
3) IEC Publications have the form of recommendations for international use and are accepted by IEC National Committees in that sense. While all reasonable efforts are made to ensure that the technical content of IEC Publications is accurate, IEC cannot be held responsible for the way in which they are used or for any misinterpretation by any end user.
4) In order to promote international uniformity, IEC National Committees undertake to apply IEC Publications transparently to the maximum extent possible in their national and regional publications. Any divergence between any IEC Publication and the corresponding national or regional publication shall be clearly indicated in the latter.
5) IEC itself does not provide any attestation of conformity. Independent certification bodies provide conformity assessment services and, in some areas, access to IEC marks of conformity. IEC is not responsible for any services carried out by independent certification bodies.
6) All users should ensure that they have the latest edition of this publication.
7) No liability shall attach to IEC or its directors, employees, servants or agents including individual experts and members of its technical committees and IEC National Committees for any personal injury, property damage or other damage of any nature whatsoever, whether direct or indirect, or for costs (including legal fees) and expenses arising out of the publication, use of, or reliance upon, this IEC Publication or any other IEC Publications.
8) Attention is drawn to the Normative references cited in this publication. Use of the referenced publications is indispensable for the correct application of this publication.
9) Attention is drawn to the possibility that some of the elements of this IEC Publication may be the subject of patent rights. IEC shall not be held responsible for identifying any or all such patent rights.

The main task of IEC technical committees is to prepare International Standards. In exceptional circumstances, a technical committee may propose the publication of a technical specification when

- the required support cannot be obtained for the publication of an International Standard, despite repeated efforts, or
- the subject is still under technical development or where, for any other reason, there is the future but no immediate possibility of an agreement on an International Standard.

Technical specifications are subject to review within three years of publication to decide whether they can be transformed into International Standards.

IEC TS 62882, which is a Technical Specification, has been prepared IEC technical committee 4: Hydraulic turbines.

Documents
Document Sharing Hub

Full document details: PD IEC TS 62882:2020

The text of this Technical Specification is based on the following documents:

Enquiry draft	Report on voting
4/375/DTS	4/398/RVDTS

Full information on the voting for the approval of this technical specification can be found in the report on voting indicated in the above table.

This document has been drafted in accordance with the ISO/IEC Directives, Part 2.

The committee has decided that the contents of this document will remain unchanged until the stability date indicated on the IEC website under "http://webstore.iec.ch" in the data related to the specific document. At this date, the document will be

- reconfirmed,
- withdrawn,
- replaced by a revised edition, or
- amended.

IMPORTANT – The 'colour inside' logo on the cover page of this publication indicates that it contains colours which are considered to be useful for the correct understanding of its contents. Users should therefore print this document using a colour printer.

Documents
Document Sharing Hub

Full document details: PD IEC TS 62882:2020

INTRODUCTION

With the increased amount of renewable energy that is being added to the electrical grid in the form of wind and solar, in addition to new energy in the form of nuclear, the grid needs to integrate more hydropower generation with flexible operation to balance loads. To meet this challenge, the hydraulic stability of the machine has become more and more important.

The current document provides a technical specification for Francis turbine pressure fluctuations. This document aims to describe pressure fluctuations, their phenomena and related problems, to define the relationship between model and prototype fluctuations, to identify methods to predict pressure fluctuations in prototypes through transposition of model measurements, and to suggest potential mitigations.

In this document, the term "turbine" refers to Francis turbines and pump-turbine operating as a turbine.

This document excludes all matters of purely commercial interest, except those inextricably bound within the conduct of the tests.

Documents
Document Sharing Hub

Full document details: PD IEC TS 62882:2020

HYDRAULIC MACHINES – FRANCIS TURBINE PRESSURE FLUCTUATION TRANSPOSITION

1 Scope

IEC 62882, which is a Technical Specification, provides pressure fluctuation transposition methods for Francis turbines and pump-turbines operating as turbines, including:

– description of pressure fluctuations, the phenomena causing them and the related problems;
– characterization of the phenomena covered by this document, including but not limited to inter-blade vortices, draft tube vortices rope and rotor-stator interaction;
– demonstration that both operating conditions and Thoma numbers (cavitation conditions) are primary parameters influencing pressure fluctuations;
– recommendation of ways to measure and analyse pressure fluctuations;
– identification of potential resonances in test rigs and prototypes;
– identification of methods, to transpose the measurement results from model to prototype or provide ways to predict pressure fluctuations in prototypes based on statistics or experience;
– recommendation of a data acquisition system, including the type and mounting position of model and prototype transducers and to define the similitude condition between model and prototype;
– presentation of pressure fluctuation measurements comparing the model turbine and the corresponding prototype;
– discussion of parameters used for the transposition from model to prototype, for example, the peak to peak value at 97 % confidence interval, the RMS value or the standard deviation in the time domain and the relation of main frequency and the rotational frequency in the frequency domain obtained by FFT;
– discussion of the uncertainty of the pressure fluctuation transposition from model to prototype;
– discussion of factors which influence the transposition, including those which cannot be simulated on the model test rig such as waterway system and mechanical system;
– establishment of the transposition methods for different types of pressure fluctuations;
– suggestion of possible methods for mitigating pressure fluctuation;
– definition of the limitations of the specification.

This document is limited to normal operation conditions. Hydraulic stability phenomena related to von Karman vortices, transients, runaway speed and speed no load are excluded from this document.

This document provides means to identify potential resonances in model test rigs and prototype turbines. Scaling-up resonance conditions are not treated in this document. When resonance exists, the transposition methods identified in this document do not apply. Under these conditions, the relationship between model and prototype pressure fluctuations cannot be determined.

This document is concerned neither with the structural details of the machines nor the mechanical properties of their components, so long as these characteristics do not affect model pressure fluctuations or the relationship between model and prototype pressure fluctuations.

AVA Documents
Document Sharing Hub

Full document details: PD IEC TS 62882:2020

2 Normative references

The following documents are referred to in the text in such a way that some or all of their content constitutes requirements of this document. For dated references, only the edition cited applies. For undated references, the latest edition of the referenced document (including any amendments) applies.

IEC 60193:2019, *Hydraulic turbines, storage pumps and pump-turbines – Model acceptance tests*

3 Terms, definitions, symbols and units

For the purposes of this document, the following terms and definitions apply.

ISO and IEC maintain terminological databases for use in standardization at the following addresses:

- IEC Electropedia: available at http://www.electropedia.org/
- ISO Online browsing platform: available at http://www.iso.org/obp

The contracting parties shall, in advance of the test, agree to clarification in writing of any term, definition or unit of measure in question.

3.1 General terms and definitions

Entry number	Term	Definition
3.1.1	Point	item established by one or more consecutive sets of readings and/or recordings at unchanged operating condition and settings, sufficient to calculate the performance of the machine at this operating condition and these settings
3.1.2	Test	collection of points that is adequate to establish the performance of the machine over a specified range of operating conditions
3.1.3	Hydraulic performance	performance parameters attributable to the machine due to hydrodynamic effects
3.1.4	Main hydraulic performance data	subset of the hydraulic performance parameters, i.e. power, discharge and/or specific hydraulic energy, efficiency, pressure fluctuation, steady-state runaway speed and/or discharge[a]
3.1.5	Additional data	subset of hydraulic performance data, which can be determined for information on the model[b]
3.1.6	Guarantees	specified performance data contractually agreed to

[a] The influence of cavitation shall be considered.

[b] The prediction of the corresponding prototype data is less accurate than that achievable for the main hydraulic performance data, due to application of approximate similarity rules.

3.2 Units

The International System of Units (SI, see ISO 80000-4 [193][1]) has been used throughout this document.

All terms are given in SI base units or derived coherent units[2]. The basic equations are valid using these units. If other units are used for certain data which are not coherent SI units, proper consideration shall be provided. Examples of non-coherent units include kilowatt instead of watt

[1] Numbers in square brackets refer to the Bibliography.

[2] $N = kg \cdot m \cdot s^{-2}$ $Pa = kg \cdot m^{-1} \cdot s^{-2}$ $J = kg \cdot m^2 \cdot s^{-2}$ $W = kg \cdot m^2 \cdot s^{-3}$

Documents
Document Sharing Hub
Full document details: PD IEC TS 62882:2020

for power, kilopascal or bar instead of pascal for pressure, min^{-1} instead of s^{-1} for rotational speed. Temperatures may be given in degrees Celsius since absolute temperatures (in kelvins) are rarely required.

Any other system of units may be used, but only if agreed in writing by the contracting parties.

3.3 Overview of the terms, definitions, symbols and units used in this document

Subclause	Title
3.3.1	Subscripts and symbols
3.3.2	Geometric terms
3.3.3	Physical quantities and properties
3.3.4	Discharge, velocity and speed terms
3.3.5	Pressure terms
3.3.6	Specific energy terms
3.3.7	Height and head terms
3.3.8	Power and torque terms
3.3.9	Efficiency terms
3.3.10	General terms relating to fluctuating quantities
3.3.11	Fluid dynamic and scaling terms
3.3.12	Dimensionless terms

Documents
Document Sharing Hub
Full document details: PD IEC TS 62882:2020

3.3.1 Subscripts and symbols

Entry number	Subscript or symbol	Definition
3.3.1.1	1	high pressure[a] section of the machine to which the performance guarantees refer
3.3.1.2	2	low pressure[a] section of the machine to which the performance guarantees refer
3.3.1.3	1', 1''.	high pressure measuring sections[b]
3.3.1.4	2', 2''.	low pressure measuring sections[c]
3.3.1.5	H	subscript denoting values related to a given head
3.3.1.6	sp	subscript denoting values of quantities such as rotational speed, discharge, etc., for which other quantities are guaranteed
3.3.1.7	max or min	subscript denoting maximum or minimum values of any term
3.3.1.8	P	subscript denoting values related to the full size machine
3.3.1.9	M	subscript denoting values related to the model
3.3.1.10	ref	subscript denoting values related to a specified reference condition
3.3.1.11	opt	subscript denoting the best efficiency point
3.3.1.12	amb	subscript referring to surrounding atmospheric conditions
3.3.1.13	pl	subscript denoting values related to the operating conditions of the prototype in the plant
3.3.1.14	R	subscript referring to runaway conditions
3.3.1.15	B	subscript referring to the runner blade of a machine
3.3.1.16	G	subscript referring to the guide vane of a machine
3.3.1.17	a	subscript referring to an axial component of force or torque
3.3.1.18	r	subscript referring to a radial component of force or torque
3.3.1.19	m	meridional direction in a rotating system
3.3.1.20	u	rotational direction in a rotating system
3.3.1.21	x, y, z	subscript referring to machine coordinates
3.3.1.22	th	subscript referring to theoretical value
3.3.1.23	h	subscript referring to hydraulic value

[a] The terms "high pressure" and "low pressure" define the two sides of the machine irrespective of the flow direction and therefore are independent of the mode of operation of the machine.

[b] Whenever possible, these sections should coincide with section 1; otherwise the measured values shall be adjusted to section 1.

[c] Whenever possible, these sections should coincide with section 2; otherwise, the measured values shall be adjusted to section 2 (see IEC 60193).

Documents
Document Sharing Hub
Full document details: PD IEC TS 62882:2020

3.3.2 Geometric terms and definitions

Entry number	Term	Definition	Symbol	Unit
3.3.2.1	Area	net cross-sectional area normal to nominal flow direction	A	m^2
3.3.2.2	Surface area	total area of a surface (of the runner, flow passages, etc.)	S	m^2
3.3.2.3	Guide vane opening	average shortest distance between adjacent guide vanes (at a specified section if necessary)	a	m
3.3.2.4	Guide vane angle	average vane angle measured from the closed position	α	°
3.3.2.5	Reference diameter	reference diameter of the hydraulic machine (see Figure 1)	D	m
3.3.2.6	Number of runner blades	number of runner blades	Z_B	-
3.3.2.7	Number of guide vanes	number of guide vanes	Z_G	-
3.3.2.8	Length scale ratio	ratio of representative prototype to model lengths[a]	λ_L	-
3.3.2.9	Level	elevation of a point in the system above the specified reference datum[b]	z	m
3.3.2.10	Dimension	corresponding model and prototype dimension	L	m

[a] In normal cases, this is the reference diameter of the machine. In cases where it is difficult to verify this reference, then another significant length may be taken.

[b] Usually mean sea level.

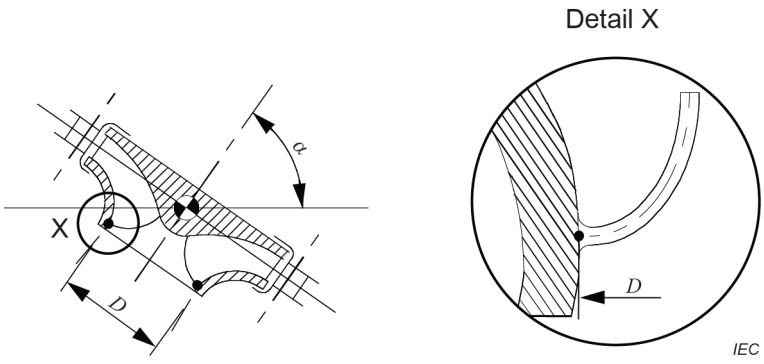


Figure 1 – Reference diameter of Francis turbine

Documents
Document Sharing Hub
Full document details: PD IEC TS 62882:2020

3.3.3 Physical quantities and properties terms and definitions

Entry number	Term	Definition	Symbol	Unit
3.3.3.1	Acceleration due to gravity	local value of gravitational acceleration at the place of testing as a function of altitude and latitude (see IEC 60193)	g	$m \cdot s^{-2}$
3.3.3.2	Temperature	temperature of water in Celsius (see IEC 60193)	θ	°C
3.3.3.3	Density	mass per unit volume of water (see IEC 60193)	ρ, ρ_w [a]	$kg \cdot m^{-3}$
3.3.3.4	Vapour pressure (absolute)	absolute partial pressure of saturated vapour in a medium where liquid and gaseous phases of a body are in thermodynamic balance[b]	p_{va}	Pa
3.3.3.5	Dynamic viscosity	quantity characterizing the mechanical behaviour of a fluid (see ISO 80000-4)	μ	Pa·s
3.3.3.6	Kinematic viscosity	ratio of the dynamic viscosity to the density of a fluid (see IEC 60193)	ν	$m^2 \cdot s^{-1}$

[a] ρ is commonly used instead of ρ_w.

[b] The vapour pressure depends only on the temperature.

3.3.4 Discharge, velocity and speed terms and definitions

Entry number	Term	Definition	Symbol	Unit
3.3.4.1	Discharge (volume flow rate)	volume of water per unit time passing through any section in the system	Q	$m^3 \cdot s^{-1}$
3.3.4.2	Mass flow rate	mass of water flowing through any section of the system per unit time[a]	(ρQ)	$kg \cdot s^{-1}$
3.3.4.3	Measured discharge	volume of water per unit time flowing through any measuring section	Q_1, or Q_2,	$m^3 \cdot s^{-1}$
3.3.4.4	Discharge at reference section	volume of water per unit time flowing through the reference section 1 or 2	Q_1 or Q_2	$m^3 \cdot s^{-1}$
3.3.4.5	Leakage flow	volumetric loss as illustrated in Figure 3	q	$m^3 \cdot s^{-1}$
3.3.4.6	Mean velocity	discharge *Q* divided by area *A* of the cross-section	v	$m \cdot s^{-1}$
3.3.4.7	Angular speed	radians per second	ω	$rad \cdot s^{-1}$
3.3.4.8	Absolute velocity	velocity measured in stationary reference frame	c	$m \cdot s^{-1}$
3.3.4.9	Peripheral velocity	peripheral velocity at the reference diameter: $u = \pi D n$	u	$m \cdot s^{-1}$
3.3.4.10	Relative velocity	velocity measured in moving (including rotating) reference frame	w	$m \cdot s^{-1}$
3.3.4.11	Rotational speed	number of revolutions per unit time	n	s^{-1}
3.3.4.12	Discharge at the best efficiency	best efficiency discharge at a given head	$Q_{opt,H}$	$m^3 \cdot s^{-1}$

[a] Both ρ and Q shall be determined at the same section and at the conditions existing in that section. The mass flow rate is constant between two sections if no water is added or removed.

AVA Documents Document Sharing Hub

Full document details: PD IEC TS 62882:2020

3.3.5 Pressure terms and definitions

Entry number	Term	Definition	Symbol	Unit
3.3.5.1	Absolute pressure	static pressure of a fluid measured with reference to a perfect vacuum	p_{abs}	Pa
3.3.5.2	Ambient pressure	absolute pressure ambient air[a]	p_{amb}	Pa
3.3.5.3	Gauge pressure	difference between the absolute static pressure of a fluid at the reference level of the pressure measuring instrument and the ambient pressure at the place and time of measurement: $p = p_{abs} - p_{amb}$	p	Pa
3.3.5.4	Peak-to-peak value of pressure fluctuation with a 97% confidence interval	difference between the maximum and minimum values of a pressure fluctuation signal which is determined with the aid of probability distribution applying counting methods and assuming a probability (e.g. 97 %). Note 1 to entry: Values occurring outside of this probability are ignored.	$\tilde{p}$	Pa

[a] Values for standard atmosphere are given as a function of elevation in IEC 60193.

3.3.6 Specific energy terms and definitions

In the International System of Units, mass (kg) is one of the base quantities. The energy per unit mass, known as specific energy, is used in this document as a primary term.

The term "head", which is energy per local unit weight, has the disadvantage that weight is a force which depends on the local value of acceleration due to gravity g, which changes mainly with latitude but also with altitude. Nevertheless, it will remain in use because it is very common. Therefore, both related energy terms are listed, the specific energy terms in 3.3.6 and head terms in 3.3.7. They differ only by the factor g.

Entry number	Term	Definition	Symbol	Unit
3.3.6.1	Specific hydraulic energy of machine	specific energy of water available between the high and low pressure reference sections 1 and 2 of the machine, taking into account the influence of compressibility (see IEC 60193)	E	$J \cdot kg^{-1}$
3.3.6.2	Suction specific potential energy of the machine	specific potential energy at section 2 corresponding to the difference between the reference level of the machine and the piezometric level at section 2 (see IEC 60193)	E_s	$J \cdot kg^{-1}$
3.3.6.3	Net positive suction specific energy	absolute specific energy at section 2 minus the specific energy due to the vapour pressure p_{va} referred to the reference level of the machine	$NPSE$	$J \cdot kg^{-1}$
3.3.6.4	Thoma number	dimensionless term indicating the conditions of cavitation under which the machine operates[a]	σ	-
3.3.6.5	Plant Thoma number	value of the Thoma number at the operating conditions of the prototype (see IEC 60193)	σ_{pl}	-

[a] It is expressed as the ratio of net positive suction specific energy NPSE to a specific hydraulic energy E (see IEC 60193).

AVA Documents Document Sharing Hub

Full document details: PD IEC TS 62882:2020

3.3.7 Height and head terms and definitions

Entry number	Term	Definition	Symbol	Unit
3.3.7.1	Net head	$H = E / g$ For the definition of E, see 3.3.6.1.	H	m
3.3.7.2	Suction height	$Z_s = E_s / g$ For the definition of E_s, see 3.3.6.2.	Z_s	m
3.3.7.3	Net positive suction head	$NPSH = NPSE / g$ For the definition of NPSE, see 3.3.6.3.	$NPSH$	m
3.3.7.4	Reference level of the machine	elevation of a point of the machine taken as reference for the setting of the machine (see Figure 2)	z_r	m
3.3.7.5	Cavitation reference level	elevation of a point of the machine taken as reference for cavitation evaluation during model tests	z_c	m
3.3.7.6	Reference level of the pressure measuring instrument	elevation of a pressure measuring device (see IEC 60193)	z_M	m
3.3.7.7	Distance between the reference level of the machine and the reference level of the instrument	$z_{rM} = z_r - z_M$	z_{rM}	m
3.3.7.8	Velocity head based on runner speed	$H_{dyn,u} = u^2/2g$	$H_{dyn,u}$	m
3.3.7.9	Velocity head based on runner speed at inlet diameter	$H_{dyn,u1} = u_1^2/2g$	$H_{dyn,u1}$	m

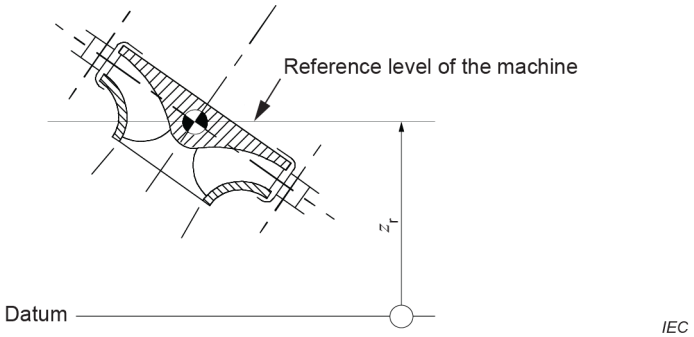
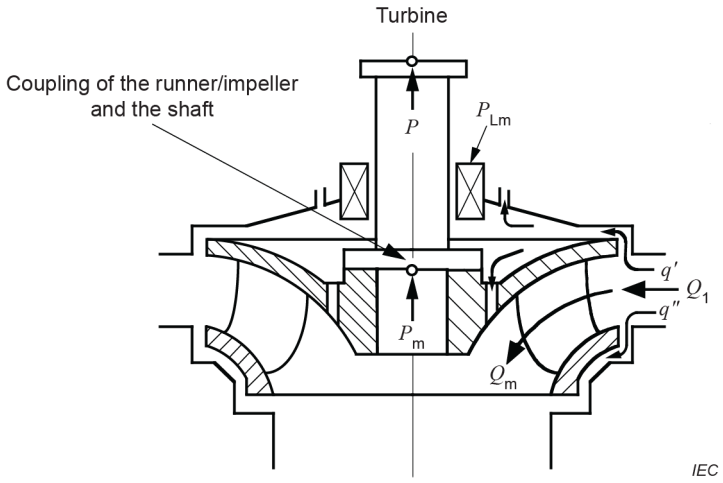


Figure 2 – Reference level of the Francis turbine

Documents
Document Sharing Hub
Full document details: PD IEC TS 62882:2020

3.3.8 Power and torque terms and definitions

Entry number	Term	Definition	Symbol	Unit
3.3.8.1	Hydraulic power	hydraulic power available for producing power: $P_h = E(\rho Q)_1$	P_h	W
3.3.8.2	Mechanical power of the machine (power)	mechanical power delivered by the turbine shaft, assigning to the hydraulic machine the mechanical losses of the relevant bearings and shaft seals (see Figure 3)	P	W
3.3.8.3	Mechanical power losses	mechanical power dissipated in guide bearings, thrust bearings and shaft seals of the hydraulic machine	P_{Lm}	W
3.3.8.4	Shaft torque	torque applied to the shaft of the hydraulic machine and corresponding to the mechanical power of the machine	T	N · m
3.3.8.5	Mechanical power of runner	mechanical power transmitted through the coupling of the runner and the shaft	P_m	W



NOTE 1

$q = q' + q''$

$Q_1 = Q_m + q$

$P_h = E(\rho Q)_1$

$P = P_m - P_{Lm}$

NOTE 2 The formulae ignore the compressibility of the water.

NOTE 3 For detailed analysis of internal losses, refer to IEC 60193.

NOTE 4 The disk friction losses and leakage losses (volumetric losses) are considered as hydraulic losses in 3.3.9.1. These "disk friction losses" are the friction losses of the outer surfaces of the runner/impeller not in contact with the flow Q_m passing the runner/impeller blades.

Figure 3 – Flux diagram for power and discharge

Documents
Document Sharing Hub
Full document details: PD IEC TS 62882:2020

3.3.9 Efficiency terms and definitions

Entry number	Term	Definition	Symbol	Unit
3.3.9.1	Hydraulic efficiency	ratio of mechanical power of the runner to the hydraulic power: $\eta_h = P_m / P_h$	η_h	-
3.3.9.2	Mechanical efficiency	$\eta_m = P / P_m$	η_m	-
3.3.9.3	Efficiency	$\eta = P / P_h = \eta_h \cdot \eta_m$	η	-

3.3.10 General terms and definitions relating to fluctuating quantities

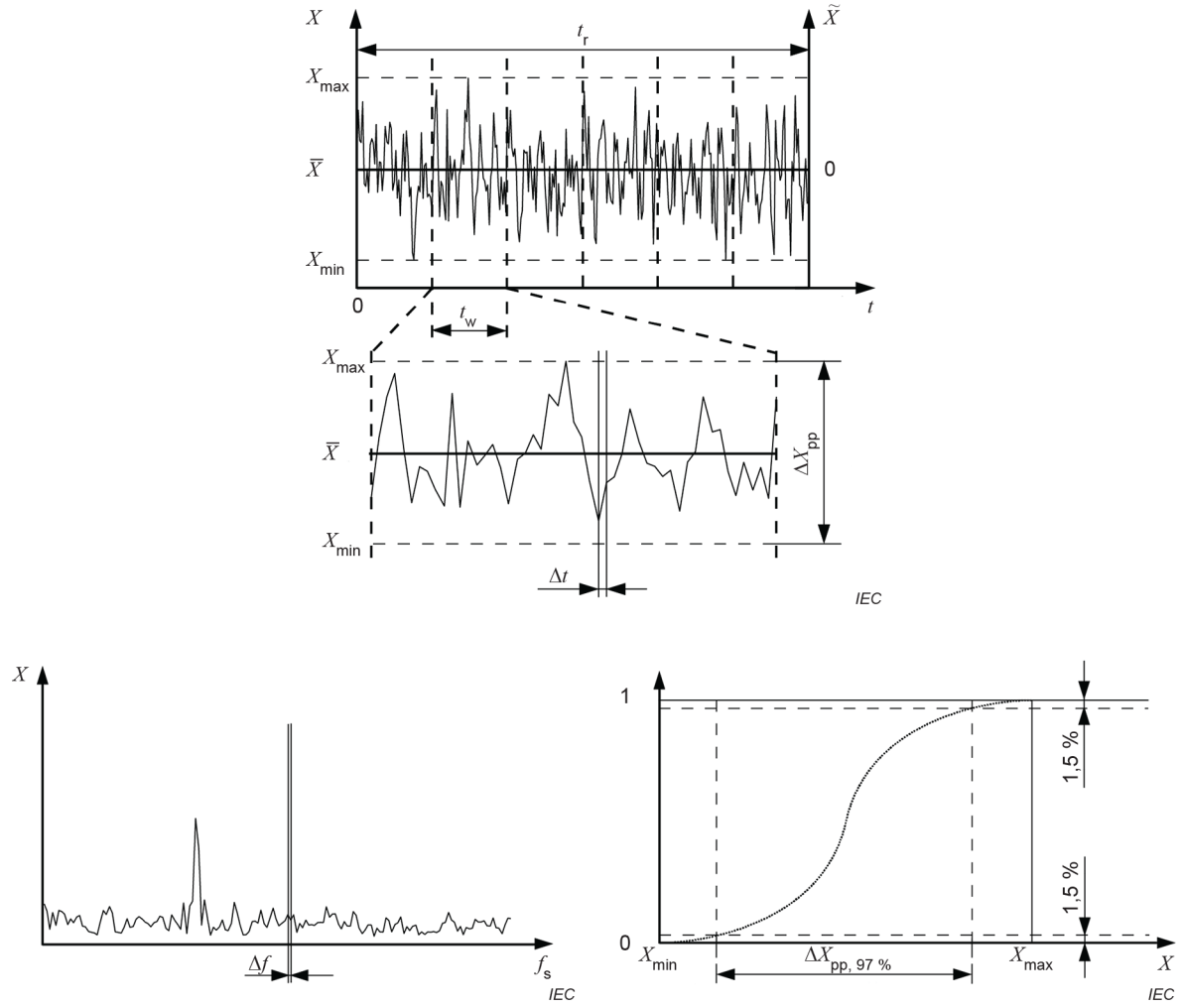
IEC 60994 and IEC 60193 provide a reference for terms relating to these quantities. The following table lists the terms relevant to this document, some of which are illustrated in Figure 4.

Documents
Document Sharing Hub
Full document details: PD IEC TS 62882:2020

Entry number	Term	Definition	Symbol
3.3.10.1	Discrete quantity	quantity represented by a sequence of its momentary values	X
3.3.10.2	Discrete quantity n	value of the quantity n	X_n
3.3.10.3	Number of samples	total number of discrete quantities	N
3.3.10.4	Number of samples in a time window	total number of discrete quantities used in the time window duration	N_w
3.3.10.5	Mean value	algebraic sum of the discrete quantities divided by the number of samples $\bar{X} = \frac{\sum_1^N X_n}{N}$	$\bar{X}$
3.3.10.6	Fluctuation of quantity	oscillatory variation of a quantity X referred to its mean value during a time interval Δt previously selected	$\tilde{X}(t)$
3.3.10.7	Maximum value	maximum value in a chosen time interval	X_{max}
3.3.10.8	Minimum value	minimum value in a chosen time interval	X_{min}
3.3.10.9	Standard deviation (effective value referred to the mean)	root-mean-square value of the deviation of a set of numbers from the mean value $\tilde{X}_{eff} = \sqrt{\frac{\sum_1^N (X_n - \bar{X})^2}{N}}$	$\tilde{X}_{eff}$
3.3.10.10	Root-mean-square value	square root of the mean value squared $X_{rms} = \sqrt{\frac{\sum_1^N X_n^2}{N}}$	X_{rms}
3.3.10.11	Peak-to-peak value	$\Delta X_{pp} = X_{max} - X_{min}$	ΔX_{pp}
3.3.10.12	Peak-to-peak value with a 97% confidence interval	difference between the maximum and minimum values of a signal which is determined using a probability distribution function for a given probability value (e.g. 97 %) Note 1 to entry: This function is estimated by applying statistical counting. The signal values outside of the corresponding confidence interval are excluded.	$\Delta X_{pp,97\%}$
3.3.10.13	Amplitude	maximum value of a sinusoidal quantity $X(t)$: $A = \frac{1}{2}\Delta X_{pp}$	A
3.3.10.14	Time	time interval	t
3.3.10.15	Sampling time interval	time interval between two consecutive samples	Δt
3.3.10.16	Frequency	inverse of period s^{-1} (Hz)	f
3.3.10.17	Sampling frequency (sampling rate)	inverse of the sampling time interval $f_s = 1 / \Delta t$	f_s
3.3.10.18	Time window duration	selected time window for frequency analyses by Fourier transform methods: $t_w = N_w \cdot \Delta t$	t_w
3.3.10.19	Frequency resolution	frequency interval between two consecutive values in the discrete Fourier transform $\Delta f = 1 / t_w = f_s / N_w$	Δf

Documents
Document Sharing Hub
Full document details: PD IEC TS 62882:2020

Entry number	Term	Definition	Symbol
3.3.10.20	Signal record time duration (acquisition time)	period of time during which a signal from a transducer is recorded (in seconds)	t_r
3.3.10.21	Synchronous pressure fluctuation	pressure fluctuation in the same phase over a cross section perpendicular to the nominal flow direction	$\tilde{p}_{syn}$
3.3.10.22	Asynchronous pressure fluctuation	pressure fluctuation phase which varies over a cross section perpendicular to the nominal flow direction	$\tilde{p}_{asyn}$



a) A pressure fluctuation signal over a defined signal recording time (t_r). A minimum of five window time lengths (t_w) shall be included in each signal record time duration.

b) The signal transformed into the frequency domain using Fourier analysis. The frequency resolution (Δf) required for each analysis is determined by the speed of rotation of the machine.

c) Using probability distribution, each measure point from Figure 4a) is cumulated, and extreme deviations from the mean fluctuation are removed. A 97 % interval of confidence is illustrated in this figure.

Figure 4 – Illustration of some definitions related to fluctuating quantities

Documents
Document Sharing Hub
Full document details: PD IEC TS 62882:2020

3.3.11 Fluid dynamic and scaling terms and definitions

Entry number	Term	Definition	Symbol	Unit
3.3.11.1	Reynolds number	ratio of inertia forces to viscous forces: $Re = D \cdot u \,/\, \nu$	Re	-
3.3.11.2	Froude number [a]	square root of the ratio of inertia forces to gravity forces: $Fr = \left[\frac{E}{gD}\right]^{1/2}$	Fr	-
3.3.11.3	Weber number [b]	ratio of inertia forces to surface tension forces: $We = \left[\frac{\rho \cdot L \cdot v^2}{\sigma^*}\right]^{1/2}$ where v is the velocity σ^* is the surface tension ρ is the density L is a linear dimension	We	-
3.3.11.4	Euler number	ratio of pressure forces to inertia forces: $Eu = \frac{\Delta p}{\rho v^2}$ where Δp is the differential pressure	Eu	-
3.3.11.5	Mach number	ratio of flow velocity to local speed of sound: $Ma = v/a$ where v is the fluid velocity a is the pressure wave propagation velocity	Ma	
3.3.11.6	Strouhal number	dimensionless number describing oscillating flow mechanism: $St = fL/v$ where $f$is the frequency of fluctuation L is the characteristic length v is the fluid velocity	St	

[a] See ISO 80000-11 [194].

[b] Other definitions of these numbers can be found in relevant scientific works.

3.3.12 Dimensionless terms and definitions

Machine performance may be characterized by dimensionless terms based on $E = 1$, $D = 1$ and $\rho = 1$ or on $n = 1$, $D = 1$ and $\rho = 1$.

The units are: H (m); D (m); E (J·kg^{-1}); n (s^{-1}); ρ (kg·m^{-3}); T (N·m); P (W); Q (m^3·s^{-1}).

The relations of these dimensionless terms to other existing definitions are given below.

Documents
Document Sharing Hub
Full document details: PD IEC TS 62882:2020

Entry number	Term	Definition	Symbol	Relations
3.3.12.1	Speed factor	$\frac{nD}{E^{0,5}}$	n_{ED}	$= \frac{1}{E_{nD}^{0,5}}$
3.3.12.2	Discharge factor	$\frac{Q_1}{D^2 E^{0,5}}$	Q_{ED}	$= \frac{Q_{nD}}{E_{nD}^{0,5}}$
3.3.12.3	Torque factor	$\frac{T_m}{\rho_1 D^3 E}$	T_{ED}	$= \frac{T_{nD}}{E_{nD}} = \frac{P_{ED}}{2\pi n_{ED}}$
3.3.12.4	Power factor[a]	$\frac{P_m}{\rho_1 D^2 E^{1,5}}$	P_{ED}	$= Q_{ED}\eta_{hT}$ (turbine) $= \frac{Q_{ED}}{\eta_{hP}}$ (pump) $= \frac{P_{nD}}{E_{nD}^{1,5}} = P_{nD} n_{ED}^3$ $= 2\pi n_{ED} T_{ED}$
3.3.12.5	Thoma number	$\frac{NPSE}{E}$	σ	$= \frac{\sigma_{nD}}{E_{nD}} = \sigma_{nD} n_{ED}^2$
3.3.12.6	Cavitation coefficient	$\frac{NPSE}{n^2 D^2}$	σ_{nD}	$= \sigma E_{nD} = \frac{\sigma}{n_{ED}^2}$
3.3.12.7	Specific speed	$\frac{nQ^{0,5}}{E^{0,75}}$	N_{QE}	$= n_{ED} Q_{ED}^{0,5} = \frac{Q_{nD}^{0,5}}{E_{nD}^{0,75}}$
3.3.12.8	Factor of pressure fluctuation	$\frac{\tilde{p}}{\rho E}$	$\tilde{P}_E$	
3.3.12.9	Coefficient of pressure fluctuation	$\frac{\tilde{p}}{\rho n^2 D^2}$	$\tilde{P}_{nD}$	
3.3.12.10	Relative discharge	$\frac{Q_H}{Q_{opt,H}}$	$Q_{H,rel}$	
3.3.12.11	Frequency coefficient	f/n	f_n	

[a] Reference is made to the mechanical power of the runner/impeller, usually measured on the model.

4 Description of pressure fluctuation phenomena

4.1 General

Pressure fluctuations are a natural occurrence in hydraulic machinery and can be of both periodic and stochastic nature. They are influenced by machine design, operating conditions and by the dynamic response of the water conduits and rotating components. Pressure fluctuations are actually a part of hydroacoustic phenomena involving unsteady pressure and flow velocity distributions. They can result in fluctuations of shaft torque, rotational speed, hydraulic loads, etc., as well as vibrations of the machine.

Low frequency disturbances are of special interest because they can propagate to the whole water conduit and the rotating parts of the electric machine.

The draft tube surge of Francis turbines and reversible pump-turbines is perhaps the most commonly identified phenomenon among low frequency pressure fluctuations. In these

AVA Documents Document Sharing Hub

Full document details: PD IEC TS 62882:2020

machines, an outlet swirl motion can develop at the runner low pressure side, inducing pressure fluctuations. In addition, cavitation can change the natural frequencies of the hydraulic system.

Turbine runners give an excitation at the rotational frequency multiplied by the number of runner blades, usually defined as the blade passing frequency. Due to the interaction of the runner blades with the guide vanes, stay vanes or spiral case, higher frequencies may be generated as multiples of the blade passing frequency.

Stochastic pressure fluctuations due to turbulent flow separation or intermittent pressure pulses due to vortex breakdown can take place in the extended operating range.

In order to deal effectively with a fluctuation issue, it is fundamental to understand the mode of fluctuation in each specific case. Table 1 shows a simplified fluctuation classification of the most common modes that will be explained in more detail through 4.2 to 4.4. Examples of typical time and frequency domain evaluations have also been added in Annex A to assist with the identification.

NOTE1 Table 1 is not a complete catalogue of all possible fluctuation modes. Some modes have been reported or proposed in various publications but are not included in the table, because they are either not very common or because they are not currently well understood.

NOTE2 m,n and k are local integers of arbitrary values in Clause 4.

Documents
Document Sharing Hub

Full document details: PD IEC TS 62882:2020

Table 1 – Pressure fluctuation overview matrix

Mode	Name	Description	Characteristics	Reference	Main concern problems	Typical mitigation
1	High load	Axisymmetric cavitating vortex rope, possibly self-excited pressure fluctuation	f_n = 0,15 to 0,5 $Q_{H,ref}$ = 1,1 to 1,5	Annex A, examples 1, 2 (Figure A.1 and Figure A.2)	Power swings Noise Fatigue in DT cone, spiral case, head cover and thrust bearing	Air admission Draft tube fins Runner cone
2	Best operation range	No rope	f_n undefined $Q_{H,ref}$ = 0,8 to 1,25	Annex A, example 3 (Figure A.3)	None, smooth operation	N/A
3	Upper part load	Draft tube cork screw cavitating vortex rope	f_n = 1 to 5 modulated by precessing rope $Q_{H,ref}$ = 0,7 to 0,95	Annex A, example 4 (Figure A.4)	Shock phenomena on draft tube wall Noise Fatigue in DT cone, spiral case and head cover Axial vibrations	Air admission Draft tube fins Runner cone
4.a	Part load	Part load stable vortex, one thread, asynchronous part	f_n = 0,2 to 0,4 $Q_{H,ref}$ = 0,4 to 0,95	Annex A, example 5 (Figure A.5)	Noise Fatigue in DT cone and head cover DT cone leakage Shaft line radial vibration	Air admission Draft tube fins Runner cone
4.b	Part load	Part load stable vortex, one thread, synchronous part	f_n = 0,2 to 0,4 $Q_{H,ref}$ = 0,4 to 0,95	Annex A, example 6 (Figure A.6)	Noise Fatigue in DT cone, runner, spiral case and penstock Axial vibrations Power swings	Air admission Draft tube fins Runner cone Power system stabilizer tuning
4.c	Part load	Part load stable vortex, several threads	f_n = (0,2 to 0,4) × (number of threads) $Q_{H,ref}$ = 0,4 to 0,6	Annex A, example 7 (Figure A.7)	Same as mode 4.a and 4.b	Air admission Draft tube fins Runner cone
5.a	Deep part load	Runner inter-blade vortices	f_n = 10 to 30 $Q_{H,ref}$ = 0,1 to 0,5	Annex A, example 8 (Figure A.8)	Runner fatigue Cavitation inside runner waterway	Air injection upstream or downstream of the runner

Documents
Document Sharing Hub
Full document details: PD IEC TS 62882:2020

Mode	Name	Description	Characteristics	Reference	Main concern problems	Typical mitigation
5.b	Deep part load	Random behaviour	Broadband excitation $Q_{H,ref}$ = 0,1 to 0,5	Annex A, example 8 (Figure A.8)	Noise Runner fatigue Shaft line torsional vibration Power swings	Air injection upstream or downstream of the runner
6.a	Rotor-stator interaction	Observed in stationary frame	$f_n = m \times Z_B$ $Q_{H,ref}$ = 0 to 1,5	Annex A, example 9 (Figure A.9)	Noise Fatigue in guide vanes, stay ring, spiral case, head cover and penstock Hydroacoustic or hydro mechanical resonance with spiral case, penstock, head cover, guide vanes and power house or parts of it	Modification of Z_B Runner blade inlet edge and guide vane shape modification Modification of vaneless zone Modification of natural frequency of structure Air injection
6.b	Rotor-stator interaction	Observed in rotating frame	$f_n = n \times Z_G$ $Q_{H,ref}$ = 0 to 1,5		Fatigue in runner Hydroacoustic resonance with runner	Modification of runner eigenfrequency Modification of vaneless zone Modification of natural frequency of structure Air injection
7.a	Speed no load	Hydro-mechanical mode, runaway operation of pump-turbines or high head turbines	f = 0,05 Hz to 0,12 Hz $Q_{H,ref}$ = ~0	Not addressed in this document	Difficult (sometimes impossible) synchronization with power network	Runner blade inlet edge modification Misaligned guide vanes Inlet valve partial closure
7.b	Speed no load	Flow separation in runner, guide vanes and stay vanes	f_n undefined Broad band excitation, random behavior	Not addressed in this document	Noise Vibration Pressure fluctuations Runner lifetime reduction	
8	Rotating stall	Pump-turbines and high head Francis turbines Interaction between runner, guide vanes and stay vanes: turbine brake operation	f_n = 0,5 to 0,7 $Q_{speed\ no\ load}$	Not addressed in this document	Stay vanes, guide vanes, runner blades and penstock pressure Radial thrust Torque oscillation	Runner blade inlet edge modification

Documents
Document Sharing Hub
Full document details: PD IEC TS 62882:2020

Mode	Name	Description	Characteristics	Reference	Main concern problems	Typical mitigation
9	von Karman vortices	Stay vanes, guide vanes or runner blades trailing edge von Karman vortices	St = 0,1 to 0,3	Not addressed in this document	Noise Fluid structure interaction and resonance Stay vanes, guide vanes or runner blade cracks Resonance with structures	Profile trailing edge modification Structural modification (detuning)

Documents
Document Sharing Hub
Full document details: PD IEC TS 62882:2020

4.2 Pressure fluctuations overview

Figure 5 shows a graphical representation of the pressure fluctuation modes that are treated in this document with corresponding discharge ranges. For a specific turbine, each fluctuation mode usually covers a smaller range than indicated in this diagram.

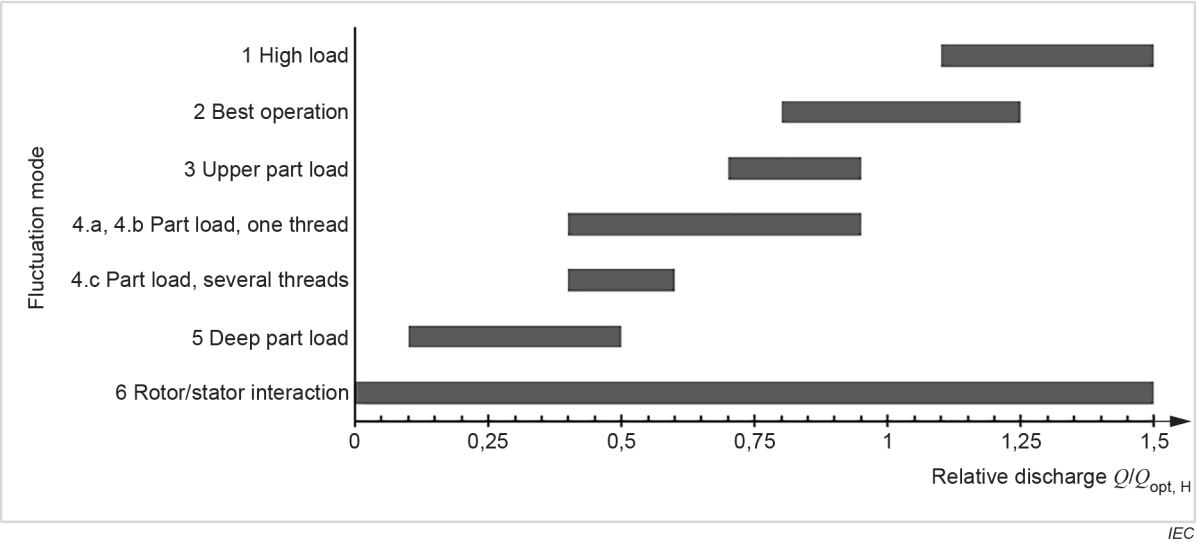
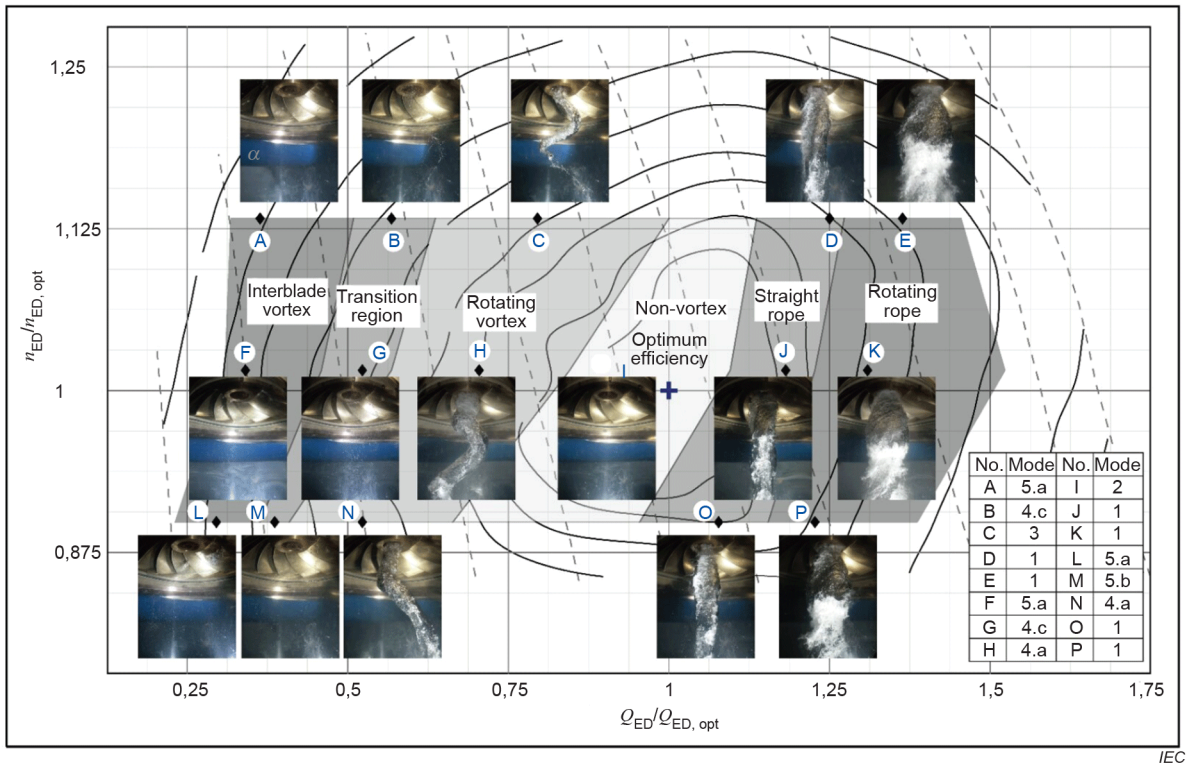


Figure 5 – Discharge range for the various fluctuation modes

Table 1 contains more detailed information for each mode. Figure 6 illustrates typical operation associated within a given mode and the corresponding location on a hill chart. Figure 7 shows a waterfall diagram of the fluctuations, which is a common way to present the data.

Documents
Document Sharing Hub
Full document details: PD IEC TS 62882:2020



No.	Mode	No.	Mode
A	5.a	I	2
B	4.c	J	1
C	3	K	1
D	1	L	5.a
E	1	M	5.b
F	5.a	N	4.a
G	4.c	O	1
H	4.a	P	1

More detailed descriptions of each fluctuation mode are provided in 4.3.

Key

— constant efficiency line

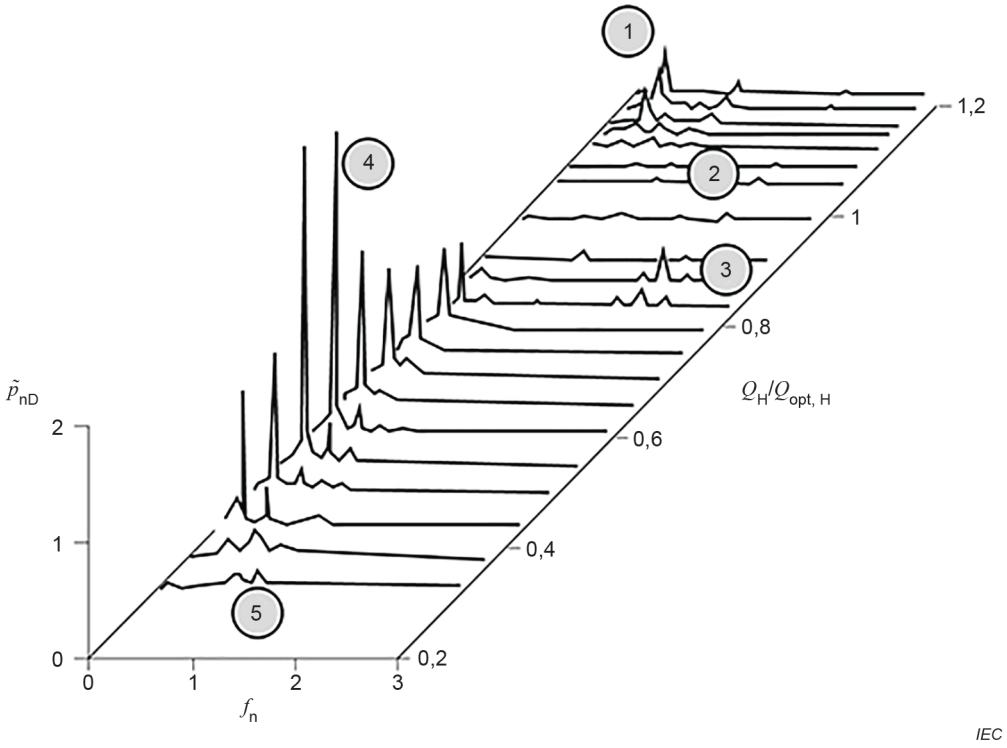
--- constant guide vane angle

\+ optimum efficiency point

NOTE A to P is operation point and draft tube phenomena; "mode" is the corresponding fluctuation mode in Table 1.

Figure 6 – Efficiency hill chart with pictures of swirling flow

Documents
Document Sharing Hub
Full document details: PD IEC TS 62882:2020



NOTE The numbers 1 to 5 correspond to the modes in Table 1.

Figure 7 – Example of a waterfall diagram of pressure amplitudes measured in the draft tube cone

4.3 General description of draft tube flow in Francis turbines

Francis turbines operating at off design conditions may present instabilities in terms of pressure, discharge, rotational speed and torque. These phenomena are strongly linked to cavitating vortex cores in the draft tube that are induced by swirling flow at the runner outlet. The absolute velocity $\vec{c}$ of the flow within the turbine can be decomposed as the sum of the peripheral velocity of the turbine $\vec{u}$ and of the relative velocity $\vec{w}$ and is given by:

$$\vec{c} = \vec{u} + \vec{w}$$

NOTE In 4.3, subscript 1 refers to the high pressure side of the runner, subscript 2 refers to the low pressure side of the runner.

Velocity triangles at the inlet and outlet of a Francis turbine runner corresponding to operation at optimum operating conditions are illustrated in

Figure 8. The absolute velocity at the outlet $\vec{c_2}$ is usually designed to be nearly axial at the best efficiency point. The influence of the discharge on the velocity triangle at the runner outlet is illustrated in Figure 9. For discharges lower than the optimum discharge, the flow at the runner outlet contains a positive (i.e. in the runner rotation direction) absolute circumferential

Documents
Document Sharing Hub
Full document details: PD IEC TS 62882:2020

velocity $\overrightarrow{c_{u2}}$, while for discharges larger than the optimum discharge, the circumferential velocity $\overrightarrow{c_{u2}}$ is negative.

As illustrated in Figure 9, the swirl below the turbine features either a precessing helical vortex rope for part load conditions or an axisymmetric vortex rope, with one or more elongated cells for full load conditions. The cavitation developing in the draft tube modifies the hydrodynamic characteristics of the draft tube flow, thereby modifying the natural frequencies of the entire hydraulic system. The volume of the gaseous vortex rope increases when the Thoma number σ is reduced. As a result, the natural frequencies of the hydraulic system decrease with the Thoma number. During part load operation, the interaction between the synchronous part of the excitation and the system natural frequencies may result in forced response hydroacoustic resonance and induce a so called draft tube surge and electrical power swing. During full load operation, the resulting axisymmetric vortex rope developing in the draft tube may, under certain conditions, start breathing as a result of the hydroacoustic system self-excitation. This phenomenon occurs when the hydraulic system damping becomes positive, resulting in a system instability. Possible resonances or system self-excitations are directly linked to the hydraulic system hydroacoustic characteristics. Their risk of occurrence therefore cannot be directly transposed from the model test to the prototype and requires specific methodologies for detailed analysis and prediction (see Annex E).

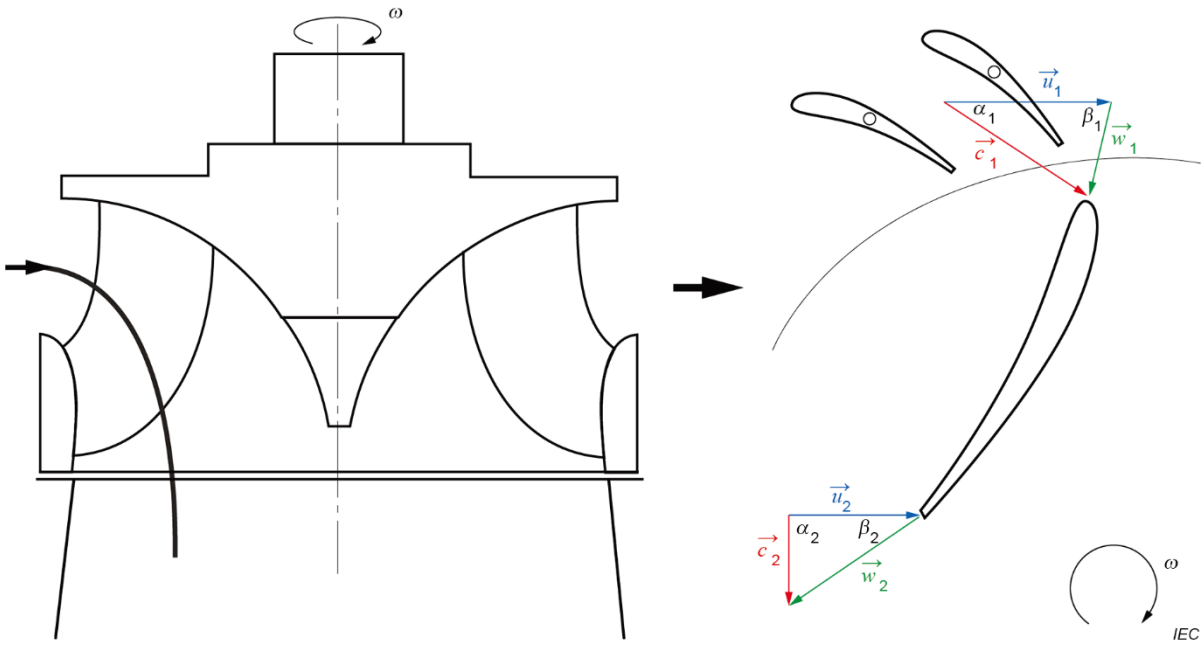


Figure 8 – Velocity triangles at inlet and outlet of the runner blade

Documents
Document Sharing Hub
Full document details: PD IEC TS 62882:2020

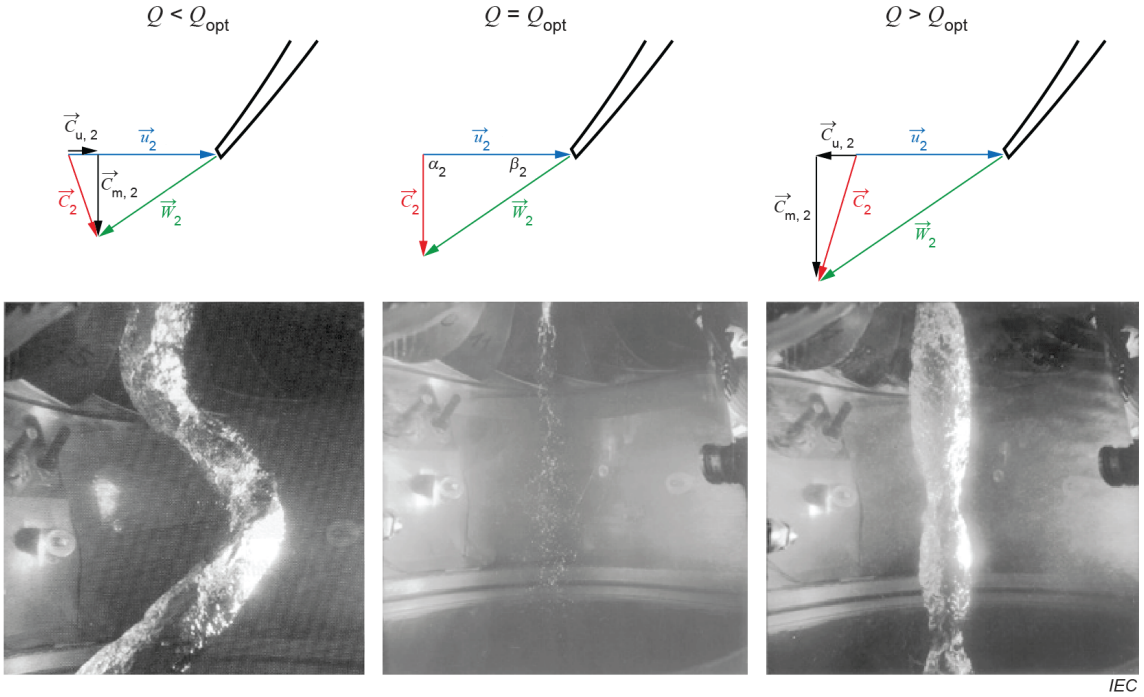


Figure 9 – Influence of the discharge on the circumferential component of the absolute velocity

4.4 Detailed description of pressure fluctuation phenomena

4.4.1 Mode 1: Pressure fluctuation in high load

4.4.1.1 General characteristics

During full or overload operation, the cavitation rope may act as an energy source under certain conditions. This leads to self-excited pressure oscillations in the whole hydraulic system. These pressure fluctuations can be harmful to the mechanical and hydraulic system. Depending on the turbine relative location in the hydraulic circuit, the turbine discharge may oscillate and generate power swings. The frequency of the pressure fluctuation is usually lower than the rotational speed and corresponds to one of the hydro acoustic system natural frequencies.

4.4.1.2 Model test examples

See Figure A.1 and Figure A.2. The positions of pressure fluctuations transducers are shown on Figure 15. This mode occurs when the turbine is operating with discharges that are larger than the best efficiency point. In this mode, the draft tube cavity has an axisymmetric shape with one or several elongated cells. There is no precession of the rope in the draft tube and therefore no asynchronous component is present, leaving only the synchronous component.

Figure A.1 shows a case corresponding to limited high load, with $Q_{H,ref}$ = 1,26. This is often close to the maximum output design limit of a prototype turbine.

Review of the frequency domain shows the 14,7 Hz (f_n = 0,85) fluctuation. There are also some overtones and undertones present, indicating that the curve shape deviates from a perfect sine wave. The fluctuation originates in the draft tube (p_1 and p_2) and travels through the guide vanes up to the spiral case with only slight reduction in amplitude, as you would expect from a synchronous fluctuation. In the vaneless zone ($p_5(1)$ and $p_5(2)$), we can also see 225 Hz, which is the runner vane passing frequency. The 225 Hz fluctuation stays only in the vaneless zone and does not travel into the draft tube or spiral case.

AVA Documents Document Sharing Hub

Full document details: PD IEC TS 62882:2020

Looking at the time domain, we see that the fluctuations in the draft tube (p_1 and p_2) are synchronous. The shapes of the time signals are very similar in the draft tube, vaneless zone and spiral case which is typical for synchronous fluctuations. The difference is that the vaneless zone fluctuations have the 225 Hz runner passing fluctuations superimposed.

In Figure A.2, we see an example of a large overload, $Q_{H,ref}$ = 1,44. This is normally far beyond the maximum output of the prototype turbine. It is nevertheless instructive to see that for this case the fluctuation amplitude in the draft tube is just as high as in high partial load.

In the frequency plane, we see the frequency 2,7 Hz (f_n = 0,15). This is a very distinct frequency, with no overtones. The amplitudes in the draft tube, vaneless zone and spiral case are the same. The vaneless zone also has the runner blade passing frequency (228 Hz) present with small amplitude.

Looking at the time domain, we see that the fluctuations in the draft tube (p_1 and p_2) are synchronous. The shapes of the time signals are very similar in the draft tube, vaneless zone and spiral case, which is also typical for synchronous fluctuations. The vaneless zone fluctuations have the 228 Hz runner passing fluctuations superimposed. It is also interesting to see the phase difference from the draft tube (p_1 and p_2) to the spiral case (p_3). The spiral case is approximately 0,03 s behind the draft tube, indicating that it takes 0,03 s for the pressure to travel from the draft tube to the spiral case. Considering that the speed of sound in a vapour/water mixture can be as low as 30 m/s, this time lag seems reasonable.

4.4.2 Mode 2: Pressure fluctuation in best operation range

4.4.2.1 General

This is an operation around the point of best efficiency at each head. During this operation, the flow in the draft tube cone is roughly axial. With little flow rotation, the centrifugal forces are small and a vapour cavity will not develop in the centre of the draft tube. Thus, the fluctuation amplitudes in the draft tube cone are generally small.

4.4.2.2 Model test examples

See Figure A.3. For this example, $Q_{H,ref}$ = 1,0. We see that the fluctuations in the draft tube, p_1 and p_2, have small amplitudes, approximately 10 % of the highest fluctuation amplitude. There is also no clear dominant frequency.

It is worth noting that the amplitude of fluctuations in the vaneless zone, p_5, is at its normal level in this mode.

4.4.3 Mode 3: Pressure fluctuation in upper part load

4.4.3.1 General characteristics

For the upper part load range pressure fluctuations may appear in the frequency range of 1 time to 5 times the runner rotational speed and feature modulations with vortex rope precession. It has been pointed out that for this particular operating point, the vortex rope features an elliptical cross section which is self-rotating.

Moreover, a "shock phenomenon" may occur in the same operating range and induce structural vibrations due to vortex rope impacts on the draft tube wall, usually in the inner part of the draft tube bend. Upper part load pressure fluctuations may also lead to resonance with the hydraulic system. In addition, the physical modulation process was identified to be related to the elliptical shape of the vortex rope cross section observed at upper part load. The motion of the elliptical vortex rope at upper part load can be decomposed into precession movement with fluctuation

Documents
Document Sharing Hub
Full document details: PD IEC TS 62882:2020

frequency ω_{rope} and self-rotation of the vortex rope with fluctuation frequency ω* as illustrated in Figure 10. From this follows the modulation process of the pressure fluctuations.

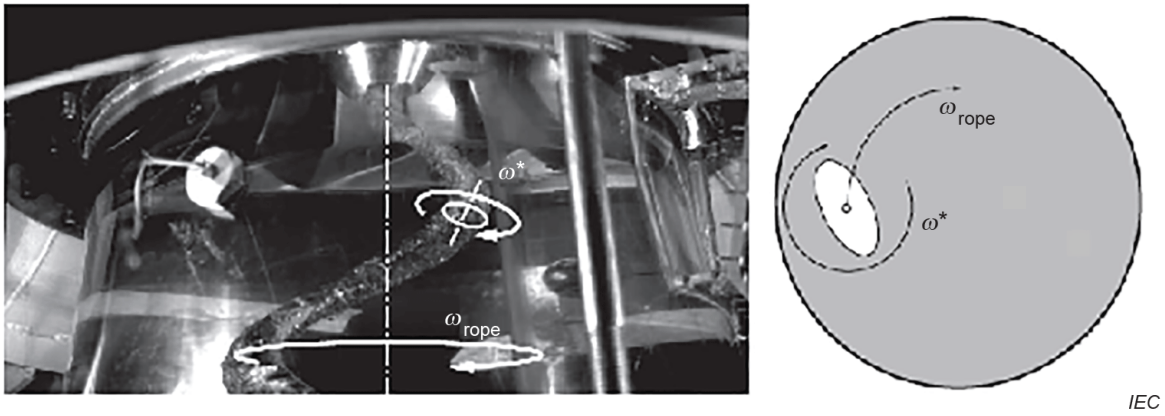


Figure 10 – Elliptical vortex rope precessing in the draft tube cone at upper part load

4.4.3.2 Model test examples

See Figure A.4. This mode is a special high frequency (f_n = 1 to 5) fluctuation produced typically at $Q_{H,ref}$ = 0,7~0,95. Other fluctuation modes, in particular mode 4, are often present together with this fluctuation.

Visually, we see a draft tube cavity, shaped like a "rope", which is rotating in the draft tube.

In Figure A.4, $Q_{H,ref}$ = 0,82. In the frequency domain, we see two dominant frequencies for p_1 and p_2. The frequency f_n = 0,3 is connected to fluctuation mode 4, while f_n = 2,0 is connected to this mode 3. As we see in the time domain, the mode 3 fluctuation is synchronous. In the frequency domain, we can thus see it at all transducer locations with the same amplitude. In comparison, we note that the mode 4 fluctuation is mainly asynchronous. Consequently, it has very low amplitude upstream of the draft tube, in p_3 and p_5.

4.4.4 Mode 4: Pressure fluctuation in part load

4.4.4.1 General

This mode is one of the most common fluctuation phenomena in hydro turbines. It can be further subdivided as indicated in 4.4.4.2 and 4.4.4.3.

4.4.4.2 Modes 4.a and 4.b – Part load

4.4.4.2.1 General characteristics

Swirling flow is defined to result from both axial and vortex motion. Increasing the swirl momentum at the inlet of the Francis turbine draft tube by reducing discharge, the draft tube flow starts from purely steady axial flow and suddenly becomes unsteady and features a precessing vortex. This phenomenon is known as the vortex breakdown and is expected when reverse flow occurs along the axis. The precessing motion of the vortex induced by the swirling flow depends on the ratio between the axial and swirl momentum and leads to pressure fluctuations with a frequency in the range between 0,2 times and 0,4 times the runner rotational frequency.

Furthermore, the pressure fluctuations in the draft tube can be decomposed into two components (see Figure 11):

a) an asynchronous component;

AVA Documents Document Sharing Hub

Full document details: PD IEC TS 62882:2020

b) a synchronous component.

The asynchronous part of the pressure fluctuations leads to unsteady pressure forces acting on the draft tube wall as well as on the runner itself and thus induces radial forces on the unit shaft line. The pressure waves induced by the synchronous part may result in hydroacoustic resonance with possible pressure fluctuations in the penstock and unit power swing. Using three pressure transducers located in a cross section of the draft tube, it is possible to determine both the asynchronous and the synchronous parts of the pressure fluctuations.

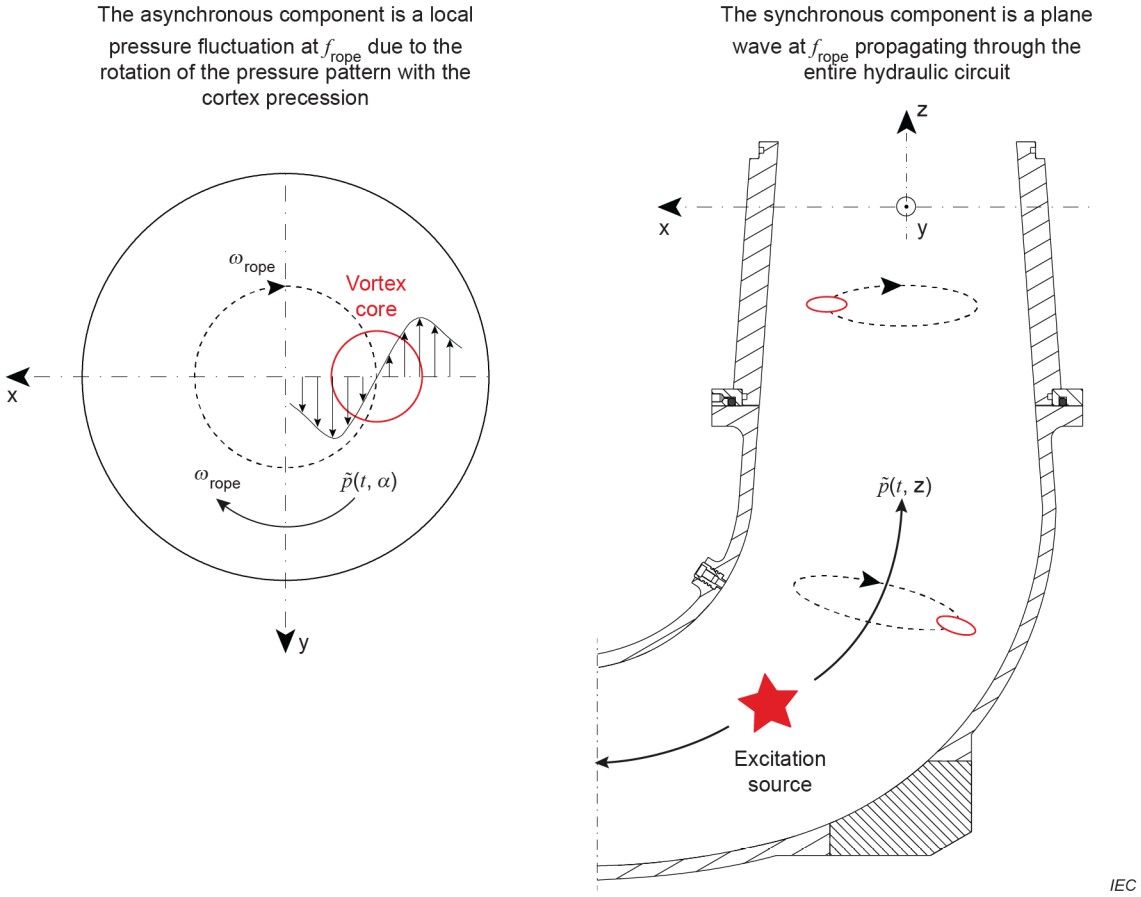


Figure 11 – Decomposition between the synchronous and asynchronous component of part load draft tube pressure fluctuations

4.4.4.2.2 Model test examples

See Figure A.5 and Figure A.6. This mode occurs when the turbine is operating with discharges below the best efficiency point, in the range $Q_{H,ref}$ = 0,4~0,95. In this mode, the draft tube cavity has a shape like a spiral shaped rope that rotates around the draft tube cone. The rotation results in an asynchronous component of the pressure fluctuation.

Figure A.5 is for $Q_{H,ref}$ = 0,63. We see a fluctuation with f_n = 0,25 and close to 180° phase difference between p_1 and p_2, which indicates asynchronous fluctuation. Even so, a smaller synchronous component can be detected and is also present as a fluctuation with the same frequency at $p_5(1)$, $p_5(2)$ and p_3. In this case, the amplitude for blade passing frequency is very small, although clearly detectable in the frequency domain for $p_5(1)$ and $p_5(2)$.

Figure A.6 is for $Q_{H,ref}$ = 0,84. For both p_1 and p_2, f_n = 0,31, but in this case the synchronous component is bigger. This explains the difference in amplitude between p_1 and p_2, as seen most clearly in the frequency domain. The amplitude for each pressure transducer depends on the

AVA Documents Document Sharing Hub
Full document details: PD IEC TS 62882:2020

phase relationship between the synchronous and asynchronous fluctuations for each particular transducer location. We also see that the blade passing frequency has high amplitude in $p_5(1)$.

4.4.4.3 Mode 4.c – Part load

4.4.4.3.1 General characteristics

This mode occurs at the low end of the part load range, typically $Q_{H,ref}$ = 0,4~0,6, where the rope in the draft tube is not stable and can disintegrate into several separate threads. Each thread will then give rise to its own fluctuation, resulting in a frequency two times to seven times higher than the frequency during operation at mode 4.a or mode 4.b.

4.4.4.3.2 Model test examples

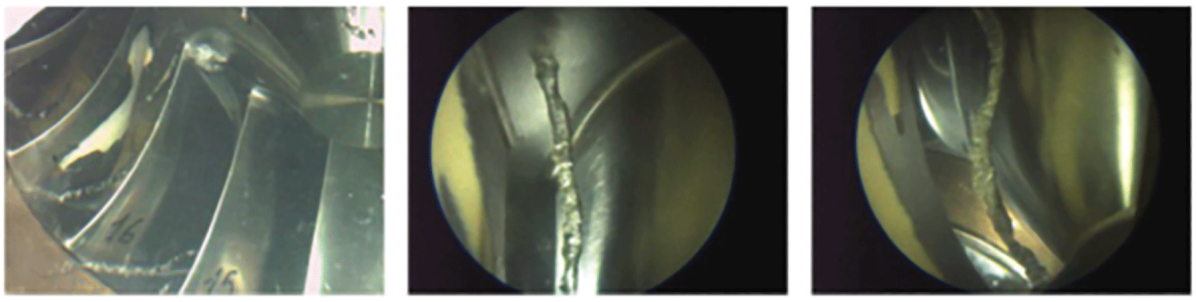
See Figure A.7, which is for $Q_{H,ref}$ = 0,50. The dominant frequency for p_1 is f_n = 1,00, while for p_2 f_n = 0,77. We also see that the frequency spectrum is much broader than for the examples with higher flow, indicating larger stochastic component. It is also difficult to identify a clear phase relationship between p_1 and p_2. Nevertheless, a small component with f_n = 0,21 can be found in p_3, indicating that a small synchronous component is present that is not connected to the formation of several threads. As expected, the blade passing frequency is clearly seen in $p_5(1)$ and $p_5(2)$.

4.4.5 Mode 5: Pressure fluctuation in deep part load

4.4.5.1 General characteristics

Decreasing the discharge of a Francis turbine by closing the guide vanes leads to an inappropriate angle of attack of the blade at the runner inlet with flow separation occurring on the blade suction side with possible recirculation in the inter-blade channel. This recirculation induces a vortex attached at the hub and extending along the blade suction side to the runner outlet close to the band. Depending on the cavitation Thoma number, cavitation appears in the vortex center (see Figure 12). Pressure fluctuations induced by the inter-blade vortex are characterized by a frequency corresponding to 10 times to 30 times the runner rotation frequency and result in force variations on the runner blades.

At deep part load, the draft tube flow features random behaviour with possible vortex rope which may appear and disappear without periodic characteristics leading to pressure fluctuations with broad frequency band. Cases are reported where the wide frequency range excited prototype shaft line torsional fluctuations that themselves induced resonance with the penstock due to rotational speed and head oscillations.



IEC

SOURCE: Yamamoto, 2016 [105]

Figure 12 – Example of inter-blade vortex

Documents
Document Sharing Hub

Full document details: PD IEC TS 62882:2020

4.4.5.2 Model test examples

See Figure A.8. The discharge for this mode is normally below the turbine continuous operating range, $Q_{H,ref}$ < 0,5. The flow in the draft tube is highly irregular and no clear frequency component is identifiable.

Figure A.8 is for $Q_{H,ref}$ = 0,25. In the frequency domain for p_1 and p_2, we see the presence of many frequencies over a large frequency range. Much of this "noise" is also present at p_3, $p_5(1)$ and $p_5(2)$. In $p_5(1)$ and $p_5(2)$, the runner blade passing frequency is present as usual.

4.4.6 Modes 6.a and 6.b: Rotor-stator interaction (RSI) pressure fluctuation

4.4.6.1 General characteristics

Francis turbines are subject to pressure fluctuations resulting from the interaction of the rotating parts and the stationary parts of the machine. This rotor-stator interaction (RSI) is the consequence of the interaction between the rotating flow perturbations caused by the runner blades and the flow perturbations caused by the guide vanes wakes (see Figure 13). This interaction induces pressure waves propagating in the entire hydraulic machine. As a result, the RSI phenomena may cause two different kinds of pressure fluctuations in the machine:

– diametrical pressure mode rotating in the vaneless zone between the guide vane and the runner blades;
– standing or travelling waves in the spiral case, also known as "phase resonance".

The first phenomenon may cause hydromechanics resonance between the rotating diametrical pressure mode and the structure of the runner or of the head cover and may induce strong vibrations, noise, crack or premature guide vanes bearing wear. The second phenomenon may cause resonance with the power house structure that generates unacceptable vibrations and noise. The standing wave phenomenon may also affect the penstock, and the interaction between the hydraulic machine and the hydraulic circuit.

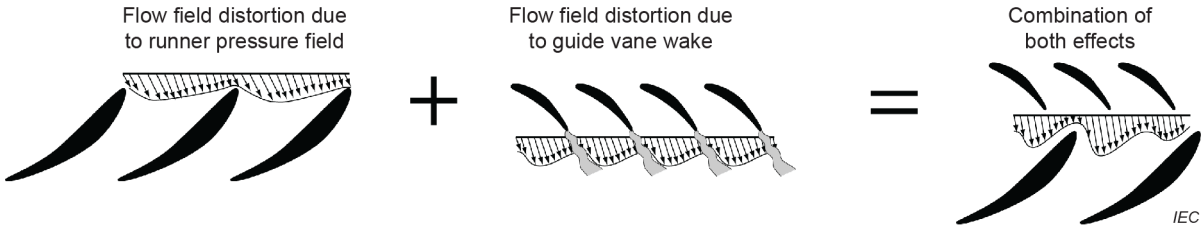


Figure 13 – Modulation process between runner blade flow field and guide vanes flow field

The diametrical mode pressure field taking place in the vaneless zone can be characterized by two modes numbers k_1 and k_2 indicating the number pressure maximum and minimum of the diametrical modes. The diametrical mode number can be computed according to the number of runner blades Z_B and the number of guide vanes Z_G defined as follows:

$$k_1 = m \cdot Z_B - n \cdot Z_G \text{ and } k_2 = m \cdot Z_B + n \cdot Z_G$$

where

m and n are integers of arbitrary values.

The diametrical mode is rotating with the respective spinning speed in the stationary frame of reference given by:

$$\omega_1 = m \cdot Z_B \cdot \omega_B / k_1 \text{ and } \omega_2 = m \cdot Z_B \cdot \omega_B / k_2$$

Documents
Document Sharing Hub
Full document details: PD IEC TS 62882:2020

Furthermore, the sign of the diametrical mode numbers k_1 and k_2 indicates that the diametrical mode is rotating in the same direction as the runner when positive, and counter-rotating when negative. It is also important to notice that lower amplitudes are expected for higher k values, because of the high harmonic number. As a result, k_2 is usually not relevant. Figure 14 presents an illustration of the meaning of the k values. It could be mentioned that a value of k = 0 leads to synchronous pressure fluctuations in the vaneless gap inducing periodic axial pressure force on the shaft line, while a value of k = ±1 leads to unbalanced rotating pressure force inducing radial force on the shaft line.

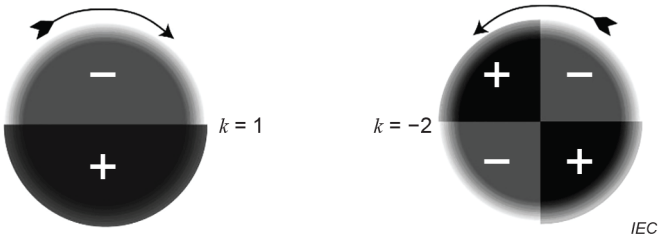


Figure 14 – Diametrical modes shapes representation according to k values

In a stationary frame of reference, the measured frequency is the runner speed times the number of blades, while in a frame of reference that rotates with the runner, the measured frequency is the runner speed times the number of guide vanes and/or stay vanes. Overtones of these frequencies may also be present.

While rotor-stator interaction is normal in all turbines, the consequences may be serious when they are in resonance with hydroacoustic and/or mechanical eigenfrequencies of turbine parts. Issues include structural failure of runner, spiral case and penstock, unacceptable noise phenomena and possible fatigue.

The RSI phenomenon is of most concern in high head Francis and pump turbines. In these types of turbines, the distance from the guide vane exit to the runner blade inlet is roughly constant over the guide vane height. As a result, the wake from the guide vane will reach the complete edge of the runner at approximately the same time. In low head turbines, the distance between guide vane and runner blade is larger and varies over the guide vane height. This means that the wake from one system will benefit from dissipation and reach the other system at different times and different tangential position at different elevations and the pressure variation will be smoothed out.

It can be noted that, since the hydroacoustic and mechanical eigenfrequencies are not directly scalable between model and prototype, the consequences of RSI phenomena cannot be directly predicted based on model tests. Nevertheless, model tests enable the measurement of the amplitude of the asynchronous pressure field in the vaneless zone, which can be used to validate or calibrate computational models for the prediction of dynamic blade loading. Moreover, measurements in the vaneless zone make it possible to determine the excitation source amplitude for both hydromechanical and hydroacoustic resonance evaluation.

It is also noted that the amplitude of this fluctuation mode is not related to runner outlet rotating speed ($\tilde{p}_{\mathrm{nD}}$) as for draft tube related phenomena, but rather to the runner inlet rotating speed ($\tilde{p}_{\mathrm{nD_1}}$). It is therefore recommended to plot this fluctuation amplitude divided by $\tilde{p}_{\mathrm{nD_1}}$ vs. the relative discharge for analysis of RSI phenomena.

4.4.6.2 Model test example

See Figure A.9, where the first diagram depicts the pressure fluctuation amplitude in the vaneless zone. The example shows the RSI fluctuation most commonly measured in model tests. It is measured in the static frame of reference and occurs for all discharges in various degrees. It comes from the pressure difference over the runner blade as it passes in front of a

AVA Documents Document Sharing Hub

Full document details: PD IEC TS 62882:2020

pressure transducer located in the head cover. Therefore, the runner blade passing frequency can be clearly identified in this fluctuation mode.

In the time domain of Figure A.9, we can note the typical "saw tooth" shape, meaning that the pressure increase is faster than the pressure decrease. This shape may also explain the overtones we can see in the frequency domain for $p_5(1)$ and $p_5(2)$. We also note that this fluctuation is localized to the vaneless zone and we do not see these frequencies in the other pressure transducers (except the 450 Hz overtone on p_3) in the frequency domain. This indicates that there is no significant hydroacoustic or mechanical eigenfrequencies in the system close to the blade passing frequency.

The RSI pressure fluctuation can also be measured in the rotating frame of reference and is then characterised by the guide vane passing frequency and its overtones. In some cases, the stay vane passing frequency may also be relevant, although this is not common.

Pressure measurements in the rotating frame of reference are uncommon. However, several instances of mechanical stress measurements on runners have identified the guide vane passing frequency.

For the guide vane passing frequency it is very important to ensure that vibrations and dynamic stresses do not exceed acceptable limits. Often this can only be achieved by avoiding hydroacoustic and mechanical resonance with the runner. Examples are known where runners have failed a very short time after commissioning due to such resonances.

5 Specifications of pressure fluctuation measurement and analysis

5.1 General

5.1.1 Overview

The purpose of Clause 5 is to detail how to measure and analyse pressure fluctuation. It is important to note that IEC 60193, IEC 60041 and IEC 60994, respectively deal with model testing, prototype testing and vibration and fluctuation measurements. Especially, in IEC 60193:2019, 7.2 is dedicated to fluctuating quantities and 7.2.2 to pressure fluctuations.

For pressure fluctuation amplitude analysis, the general use of a 97 % confidence interval is recommended to ensure mutually comparable results. The standard deviation may also be accepted if relevant parties agree.

Consequently, Clause 5 will underline the important points to take from these standards and complement them.

5.1.2 Purpose of the measurements

Generally, pressure fluctuation measurements are realized with the ultimate objective to have a prototype operating in stable conditions, free of harmful vibrations and with dynamic stress levels compatible with the expected useful life of the machine. Model testing is mainly done to document the design status with the objective of predicting the prototype behaviour and its stability by comparison with similar models.

According to IEC 60193, the main measurements that shall be carried out on the model are the following:

– relative magnitude of the pressure fluctuations within a specified operating range;
– nature of the pressure fluctuations, periodic or stochastic;
– dominant frequency of the pressure fluctuations, if any;

Documents
Document Sharing Hub
Full document details: PD IEC TS 62882:2020

– effect of corrective methods such as air admission (effectiveness and suitable location);
– intensity of the pressure fluctuations of the model compared with other models of similar specific speed.

Even though transposition of model test results is seen to have a good predictability for some phenomena, it is likely to encounter differences on prototype. It is therefore a good practice to measure these values on the prototype even if the prototype is operating with acceptable levels of vibration or if the model was operating smoothly. This could help underline problematic operating conditions which seemed normal at first.

In cases of a rough operating machine or wide operating range, for example with pressure fluctuation values above the guaranteed values, a detailed analysis shall be done. Dynamic measurements and pressure fluctuations measurements should be considered.

The prototype detailed analysis test covers the same type of measurements, except that there is usually no comparisons with models other than the homologous one.

In cases with bad accessibility, other dynamic measurement methods can be performed to supply root cause analysis.

5.1.3 Procedures and parameters to record

5.1.3.1 Model test

On the model, the test points should cover at least the specified discharge operating range under constant test specific hydraulic energy values and at least the minimum Thoma number for a given head or operating condition. The test head values often relate to prototype specific maximum and minimum operational heads and one or several rated operational heads in plants with large variations of specific hydraulic energy. A sufficient number of guide vane openings should be explored, particularly at part and full-discharge, to characterize in detail the fluctuation phenomena that occur with changes in the operating conditions. Knowing that upper part load happens in a narrow range of guide vane opening, the number of test points shall be higher where this phenomenon is expected.

5.1.3.2 Prototype measurement

On the prototype, the overall view of the pressure fluctuations is obtained by recording a sufficient number of test points between speed no load and full guide vane opening (at least every 5 % of rated power). Another way to obtain the big picture is by ramping up or down the guide vane opening sufficiently slowly (0,1 %/s on the servo-motor stroke) over the domain of operation. The latter is faster but known to give pressure fluctuation amplitudes different than those obtained by maintaining a constant guide vane opening. Moreover, depending on the chosen servo-motor slope, the apparition of the phenomenon can switch in flow (lag) or not happen at all. Thereafter, an additional number of test points at a constant guide vane opening can be performed near the limits of the normal operating range or contractual limits, and where amplitude of pressure fluctuation changes rapidly with flow. For each test point, the guide vane opening shall be constant to avoid flow or head variation due to load-frequency control. If possible, the head should be modified by starting/stopping adjacent units to measure its impact on important pressure fluctuation test points.

For standard checks of pressure fluctuations, in case of locally high vibrations, the unit shall be operated in this critical zone. The phenomenon shall be caught when it clearly occurs. The turbine should be measured in small steps of guide vane openings in and around this region, also by varying the surrounding conditions. Surrounding conditions may be including operation of other parallel machines, varying the tail water level and so on. Measurement transducer location shall be taken, as far and as available on the prototype.

In a less complex version to check the guarantees in sensitive operating points of a strong vibrating unit, the site measuring range should depend on the problem, the size and the accessibility of the prototype.

AVA Documents Document Sharing Hub

Full document details: PD IEC TS 62882:2020

Besides the pressure fluctuation signals, the following parameters should be recorded at the same time:

– the head/specific hydraulic energy;
– the rotational speed;
– the trigger signal (for phase angel calculation)
– the absolute discharge or relative discharge by Winter-Kennedy method;
– the unit power;
– the upstream water level and downstream water level, the latter being used to determine the Thoma number;
– the water temperature;
– the air discharge measurement for air admission;
– the guide vane opening and/or angle, servomotor stroke;
– the axial loads (optional);
– the shaft line radial displacement

5.1.4 Locations of pressure fluctuation test transducers

The location of pressure transducers should consider the need to capture all phenomena mentioned in Clause 4. Figure 15 shown below is based on IEC 60193:2019, Figure 90, which proposes a location for these transducers.

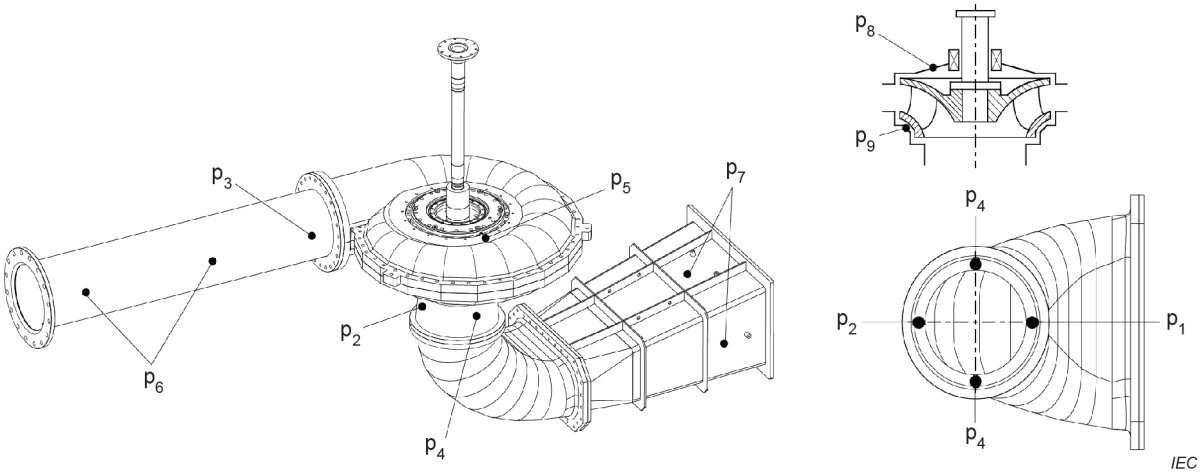


Figure 15 – Suggested locations of pressure transducers

Table 2 describes each transducers location shown in Figure 15 and links those locations to the phenomena listed in Table 1 they are intended to measure.

Documents
Document Sharing Hub
Full document details: PD IEC TS 62882:2020

Table 2 – Locations of pressure fluctuations transducers

Locations	Locations description	Mode in Table 1	Important content
p_1	Draft tube cone downstream 0,3∼1,0 D2 from the runner exit	1~5	Key
p_2	Draft tube cone upstream 0,3∼1,0 D2 from the runner exit	1~5	Key
p_3	Spiral case	1, 2 ,3, 4.b	Key
p_4	Draft tube cone 90° apart from p1 or p2, preferably two locations, the same section with p1 and p2	1~5	Optional
p_5	Vaneless zone, preferably two locations, upstream and downstream at the same diameter	6.a	Key
p_6	Penstock	1, 3, 4.b	Optional
p_7	Draft tube outlet	1~5	Optional
p_8	Head cover	6.a	Optional
p_9	Discharge ring	1 ,4, 6.a	Optional

For the purposes of this document, the measurement of p_1, p_2, p_3 and p_5 is necessary to determine the hydraulic excitation and is identified as key locations in Table 2. These locations also cover the main phenomena for which transposition is foreseen.

P_4 is important to confirm the rope rotation direction. It also adds precision to the amplitude and phase measurement. However, the rope rotation direction is predictable from the runner rotation direction. Also, p_1 and p_2 are sufficient to compute the phase difference. Therefore, it is not considered as necessary.

Other locations can be considered as optional. They can be used to add data and study the wave propagation in the waterway (p_6 and p_7) and around the runner (p_8 and p_9). Therefore, these locations could help doing more complex analysis such as resonance prediction.

IEC 60193 suggests that p_1 and p_2 are placed 0,3 diameter length to 1,0 diameter length from the low pressure side of the runner. There is a great margin between both values and pressure fluctuation measurement could vary noticeably from one elevation to the other. In order to compare adequately the model and prototype values, it is important to have the sensors at the same relative level, for example both at 0,3 times the runner diameter.

A typical location for p_5 is at mid-distance between the diameter of the guide vane outlet at full opening and the outer runner diameter at the crown.

5.1.5 Data acquisition for pressure fluctuation measurements

The fact that pressure fluctuation is a dynamic phenomenon brings additional complexity in term of data acquisition requirements. The system shall take into account the range of frequency that shall be measured and should prevent potential noise to distort the signal. The range measured frequency should allow cover of all the phenomena mentioned in Table 1.

Most of the information about signal conditioning, analog to digital conversion, sampling rate, duration of signal record, frequency resolution and phase information is important and discussed thoroughly in IEC 60193:2019, 7.2.1.2. The principles mentioned in this document apply to both model and prototype.

Documents
Document Sharing Hub
Full document details: PD IEC TS 62882:2020

It is recommended to use a system that allows having synchronous measurement in all channels or show a negligible delay (less than ±10° for the phase) between channels with respect to the phase difference at the frequency of interest. An example of such a system can be found in IEC 60193.

The maximum permissible error of the measuring chain shall be smaller than ±5 % of the maximum measured value.

5.1.6 Transducers and calibration

As for the data acquisition system, pressure transducers and calibration methods shall be chosen considering the dynamic nature of pressure fluctuations. Frequency response and sensitivity are amongst the most important parameters to look at. Pressure transducers type, calibration and installation are discussed in IEC 60193:2019, 7.2.2.3 and 7.2.2.4. The principles mentioned in this document apply to both model and prototype.

An important parameter to consider in the installation is the need to have a mounting allowing the sensor membrane to be flush with the hydraulic profile. Any chamber created between the sensor and the point of measurement can trigger resonances phenomena that will pollute the signal. This requirement can sometimes be hard to meet, especially on the prototype. Subclause 5.3 gives some information and references about these cases.

Typical parameters about pressure fluctuation transducers are shown in Annex B.

In addition, three typical calibration methods for dynamic pressure transducers are shown in Annex C.

5.2 Pressure fluctuation on a model turbine

5.2.1 General

As previously mentioned, IEC 60193 adequately covers model pressure fluctuation testing. Any test should comply with IEC 60193:2019 and more specifically with 5.1 and 7.2.2.

Requirements such as those mentioned in IEC 60193:2019, 5.1, and the operating ranges to be tested are treated adequately in IEC 60193.

Figure 16 shown below is based on IEC 60193:2019, Figure 92, and provides a good example on how to explore the operating range of a machine.

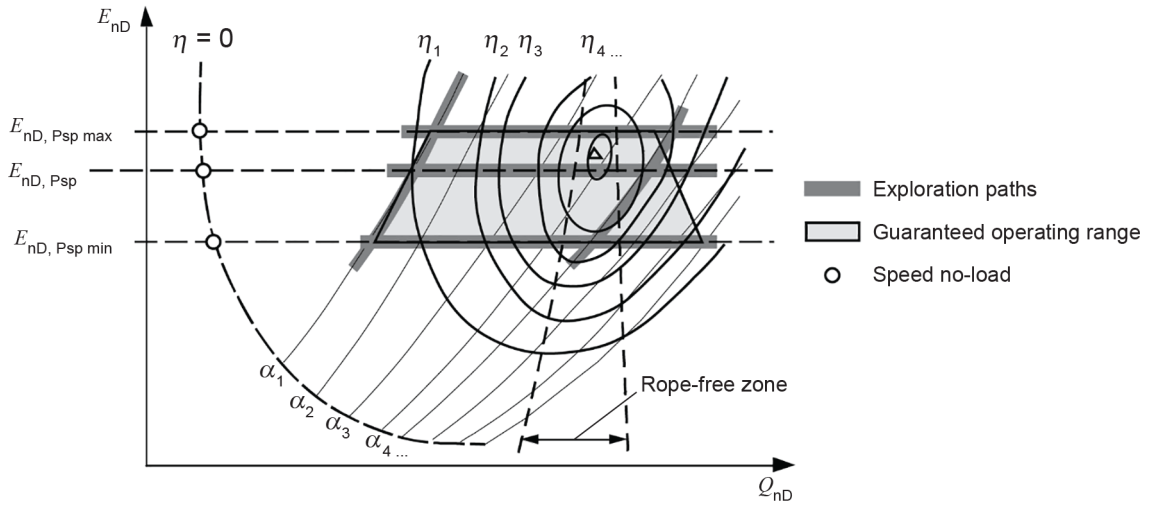


Figure 16 – Turbine hill-chart with exploration paths

Documents
Document Sharing Hub
Full document details: PD IEC TS 62882:2020